2014-12-01

Algebraic Semi-Classical Model for Reaction Dynamics

Tim Glenn Wendler
Brigham Young University - Provo

Algebraic Semi-Classical Model for Reaction Dynamics

Tim Wendler

A dissertation submitted to the faculty of
Brigham Young University
in partial fulfillment of the requirements for the degree of

Doctor of Philosophy

Manuel Berrondo, Chair
Scott D. Bergeson
Gus L. W. Hart
J. Ward Moody
Jean Francois S. Van-Huele

Department of Physics and Astronomy

Brigham Young University

December 2014

ABSTRACT

Algebraic Semi-Classical Model for Reaction Dynamics

Tim Wendler
Department of Physics and Astronomy, BYU
Doctor of Philosophy

We use an algebraic method to model the molecular collision dynamics of a collinear triatomic system. Beginning with a forced oscillator, we develop a mathematical framework upon which inelastic and reactive collisions are modeled. The model is considered algebraic because it takes advantage of the properties of a Lie algebra in the derivation of a time-evolution operator. The time-evolution operator is shown to generate both phase-space and quantum dynamics of a forced oscillator simultaneously. The model is considered semi-classical because only the molecule's internal degrees-of-freedom are quantized. The relative translation between the colliding atom and molecule in an exchange reaction $(\mathrm{AB}+\mathrm{C} \rightleftharpoons \mathrm{A}+\mathrm{BC})$ contains no bound states and any possible tunneling is neglected so the relative translation is treated classically.

The purpose of this dissertation is to develop a working model for the quantum dynamics of a collinear reactive collision. After a reliable model is developed we apply statistical mechanics principles by averaging collisions with molecules in a thermal bath. The initial Boltzmann distribution is of the oscillator energies. The relative velocities of the colliding particles is considered a thermal average. Results are shown of quantum transition probabilities around the transition state that are highly dynamic due to the coupling between the translational and transverse coordinate.

Keywords: algebraic, reaction, dynamics, quantum, anharmonic, triatomic, collinear

ACKNOWLEDGMENTS

I want to thank my wife Melanie for supporting me. I also wish to thank Manuel Berrondo, Jean-François Van Huele, and Scott Bergeson for reviewing this document and for ripping it to shreds as every good advisor should do to a thesis draft. Thank you so much to Michael Ware and Shelena Shamo for helping me with the formalities of this document.

Contents

Chapter 1

Introduction

1.1 Dissertation Goals and Results

The main goal of this dissertation is to model anharmonicity in reactive collisions. To achieve this I build on two smaller goals: modeling the quantum dynamics of a driven anharmonic oscillator and modelling inelastic collisions between an atom and a diatomic molecule. These goals are achieved by exploiting algebraic properties of the time-evolution operator and the use of a mean-field theory.

An additional goal is to apply the inelastic and reactive models to a statistical distribution of collisions. An ensemble of molecular vibrations obeying a Boltzmann distribution rearrange after collisions with thermally averaged incoming atoms. The results of iterating this model in an attempt to represent a Boltzmann distribution are shown as a transition probability landscape. This landscape plot is essentially the time-dependent analysis of the transition probabilities in a molecular collision model.

1.2 Methods Used

I use Lie algebras to solve the Time-Dependent Schrödinger Equation. The time-evolution operator is expressed as a product of exponentiated quantum mechanical operators. The operators are associated with the observables of interest which in this case are position, momentum, and energy. I also use a mean-field theory when introducing an anharmonic potential which is essentially composed of higher-order operators not in the original algebra.

1.3 My Specific Contributions

My contribution comes from the results of constructing both an inelastic and reactive collision Hamiltonian with the Lie algebra approach. I simultaneously plot transition probabilities and phase-space trajectories throughout the excitation. The "landscape" plots showing the quantum dynamics of a bath of molecules leaving a Boltzmann distribution are visualizations in reactive collision theory that are my most unique contribution.

Another important contribution of mine is obtaining results such as resonances in the trajectories and population inversion of the transition probabilities in an exchange reaction: $A + BC \rightarrow AB + C$. These results show that the algebraic model reveals quantum dynamic details around the reaction transition state not seen in the literature. The model can predict state-to-state transition probabilities continuously throughout the whole reaction. Its accuracy as a model is mainly due to the coupling of the translational and transverse coordinate. Previous work [1–3] assumes pre-calculated trajectories or just produced asymptotic state-to-state probabilities without coupling the translational and transverse coordinate, neither of which truly reveal and resolve the quantum dynamic details around the transition state of a collinear triatomic exchange reaction.

1.4 New Results as Compared with Earlier Approaches

This model exploits the Hamiltonian as a generalized algebraic entity which has the potential to obviate numerical error in quantum dynamics. We simultaneously analyze an oscillator's motion with its quantum dynamics continuously throughout external interaction, with a more unified model than what we've seen in the literature [4–6]. The model also is the first to resolve the quantum dynamic details of a bath of molecules as they leave equilibrium through collisional energy transfer. This model contains specific prediction potential as it is generalized to be able to compare to femtochemistry experiments, lasing, and nuclear reactions by specifying only a handful of parameters. Perhaps the most profound result from this work is the fact that we can predict state-to-state transition probabilities of an inelastic collision or a reaction directly from classical trajectories.

1.5 Description of Major Sections

In Chapter 2 I address the forced quantum oscillator and its similarity to inelastic atom/molecule collision systems. I use a Lie algebriac approach and discuss how it is the foundation upon which the molecular collision model is built. Chapter 3 covers the application of Lie algebra to collinear triatomic inelastic atom/molecule collisions. Chapter 4 is where the main goal of modeling a collinear triatomic exchange reaction is presented in detail.

Appendix A contains 4 separate computer codes that were used to generate the results of the model as it developed from forced oscillator to reactive collision. Appendix B contains a relevant background of molecular collision theory. This background includes specific motivations for my approach to the reactive molecular collision. Appendix C explains quantum dynamic nuances that are important in fully understanding the model's results. Appendix D shows derivations of standard algebraic expressions and explains mathematical details not shown in the main chapters.

Chapter 2

The Forced Oscillator with Lie Algebra

My initial goal is to model the exchange of energy between a quantum harmonic oscillator and a time-dependent external driving field, using an algebraic approach. I start with the time-dependent Hamiltonian $\hat{H}(t)$ for a driven quantum oscillator. I then find a suitable Lie algebra with which the Hamiltonian may be expressed. This is done with linear combinations of the Lie algebra basis elements which belong to the set $\{\hat{a}^\dagger, \hat{a}, \hat{N}, 1\}$ where $\hat{a}^\dagger$ and $\hat{a}$ are the ladder operators, and $\hat{N} = \hat{a}^\dagger \hat{a}$ is the number operator for the harmonic oscillator. I also construct a generalized time-evolution operator $\hat{U}(t)$ with the same set of basis elements. When $\hat{H}(t)$ and $\hat{U}(t)$ are used in the Schrödinger equation, the linear independence of these elements allows us to equate their coefficients and get four quantum equations-of-motion. The solutions to these equations give the time-evolution operator the explicit form needed to simultaneously calculate both transition probabilities and phase-space trajectories given the initial conditions of a driven quantum oscillator system.

The mathematical foundation is based on the forced quantum harmonic oscillator which has been solved many times and in many ways. My contribution comes from the Lie algebra point of view. I simultaneously analyze the oscillator's motion, and its quantum dynamics continuously throughout the external interaction with a more unified model than what is seen in the literature.

The forced quantum harmonic oscillator is the launching pad for my work with molecular collisions in the next chapter. My work is generalized and readily available for the modeling of any system that includes an exchange of energy between a quantum oscillator and a time-dependent external driving field. The model has the potential to apply to femtochemistry experiments, lasing, and nuclear reactions by specifying only a handful of parameters.

My next goal is to introduce an anharmonic potential and I find it is necessary to use a set with 5 elements, $\{\hat{a}^\dagger, \hat{a}, \hat{N}, \hat{N}^2, 1\}$, along with a mean-field theory as this set is not closed under commutation. I use as a model a Morse potential where the algebra element is exponentiated. The expansions necessary for the Hamiltonian to be a linear combination of the 5 elements are noted as a limiting factor in the model.

There are two ideas which need to be explained in detail for this dissertation. The first is the forced oscillator [7, 8] upon which the whole reactive collision model is built. The second is the Wei-Norman Ansatz [9] to the Schrödinger equation. This chapter is focused on making those concepts clear to the reader, in order to prepare them for the next chapters, where the model is applied to molecular collisions.

2.1 The Foundation for Quantum Dynamics

The first challenge we come across when modeling a forced quantum oscillator is time-dependence. Time-dependence in the potential of a quantum Hamiltonian introduces a host of mathematical issues. We found it most helpful to research the origins of these issues in the Schrödinger picture. Starting with the time-dependent Schrödinger equation for the time-evolution operator

$$i\hbar \frac{d\hat{U}(t,t_0)}{dt} = \hat{H}(t)\,\hat{U}(t,t_0), \tag{2.1}$$

we end up with three general cases for time-evolution of a quantum system. These depend on the

Hamiltonian's time-dependence. These cases are as follows:

CASE 1 The Hamiltonian operator is independent of time. When the parameter of time is changed, the Hamiltonian remains unchanged. The time-dependent Schrödinger equation for the time-evolution operator is then easily solved for,

$$\hat{U}(t,t_0) = e^{-\frac{i}{\hbar}\left[\hat{H}(t-t_0)\right]}. \tag{2.2}$$

An example of this case is a harmonic oscillator.

CASE 2 The Hamiltonian operator depends on time, but $\left[\hat{H}(t_1),\hat{H}(t_2)\right] = 0$ for *any* t_1 and t_2.

$$\hat{U}(t,t_0) = e^{-\frac{i}{\hbar}\int_{t_0}^{t}\hat{H}(t')dt'}. \tag{2.3}$$

There are few systems where this case applies. One example would be a spin-magnetic moment subjected to a magnetic field whose strength varies with time but whose direction remains the same.

CASE 3 The Hamiltonian operator depends on time, but $\left[\hat{H}(t_1),\hat{H}(t_2)\right] \neq 0$ for *some* t_1 and t_2. Appendix C.4 shows explicitly why this is an issue. An example of this case is an oscillating charge in a time-dependent external electric field $f(t)$. In this system $\left[\hat{H}(t_1),\hat{H}(t_2)\right] \rightarrow [f(t_2)-f(t_1)]\left(\hat{a}^\dagger - \hat{a}\right) \neq 0$ for *any* t_1 and t_2. The formal solution for this case is the Dyson series,

$$\hat{U}(t,t_0) = 1 + \sum_{n=1}^{\infty}\left(\frac{-i}{\hbar}\right)^n \int_{t_0}^{t} dt_1 \int_{t_0}^{t_1} dt_2 ... \int_{t_0}^{t_{n-1}} dt_n \hat{H}(t_1)\hat{H}(t_2)...\hat{H}(t_n). \tag{2.4}$$

Another example of CASE 3 is the quantum dynamics of an inelastic collision, where the Hamiltonian does not commute with itself at different times as well. A simple model of inelastic collisions can be founded upon a Hamiltonian of the following form

$$\hat{H} = \hbar\omega\left(\hat{a}^\dagger\hat{a} + \frac{1}{2}\right) + f(t)\,\hat{a} + f^*(t)\,\hat{a}^\dagger. \tag{2.5}$$

This is analogous to a harmonic oscillator (diatomic molecule), in a time-dependent "dipole field" (colliding atom). This form works well on either side of the collinear triatomic reaction (A+BC or AB+C) separately. This similarity between the Hamiltonian for a forced oscillator and the Hamiltonian for an inelastic collision [10–12] is why we base our model here. For reactions however, notice the transition state is not accessible yet, connecting the two systems smoothly is an ultimate challenge we address later.

I do not calculate any dynamics here but rather want to emphasize the power of the time-evolution operator $\hat{U}(t,t_0)$. All quantum dynamics of interest are found with it. Using the Ehrenfest theorem, I show how we can explore the phase-space dynamics with the time-evolution operator. I also show how to find quantum state transitions with $\langle n|\hat{U}(t,t_0)|m\rangle$, where n and m are the initial and final quantum numbers of the oscillator. The role of the time-evolution operator is central in quantum dynamics.

The traditional approach for the theory of quantum dynamics of molecular collisions does not involve the time-evolution operator. It is common to focus on the time-dependence of the wave functions and not on the operators. Wave functions are not central to our calculations. Instead, we use an algebraic approach. The general idea of quantum algebras has been around since the early 20th century. The idea of quantum dynamics using perturbations came soon after, though it focused on wave function expansions. In 1963, James Wei and Edward Norman's, "Lie Algebraic Solution of Linear Differential Equations" was an important step towards using algebra to simplify quantum dynamics. The Wei-Norman [9] result for the time-evolution operator can greatly simplify the calculations for time-dependent systems. The method focuses on the time-evolution operator and does not use wave functions or perturbative expansions. It relies on number states and ladder operators. This is our motivation for using the time-evolution operator to model the quantum dynamics of a reactive collision in this dissertation.

2.2 The Forced Quantum Oscillator

The forced quantum oscillator or "dipole field", is the core model of what I am doing. I am building on the dipole field model because it applies to an oscillating molecule in the presence of an incoming atom. This problem involves a harmonically oscillating charge in the presence of an external time-dependent field. This model has a history we can build on [13]. We refer to a quantum mechanics textbook [7] first.

Three "pictures", or mathematical formalisms arise in traditional quantum dynamics. In the Heisenberg picture, one keeps the states constant and lets the operators evolve in time. The Schrödinger picture in contrast lets the states evolve while the operators stay constant. The third picture, called the interaction picture, is a mix of the other two. When applying a fourth, more modern Lie algebraic approach, it is useful to make a rigorous comparison with the three traditional pictures to see exactly what is new and advantageous about the approach.

The Heisenberg picture, Lie Algebra and Interaction picture all overlap at some point. It is not always clear which is most appropriate for the quantum system in question. In the Heisenberg picture where the states are constant and the operators, $\hat{x}$,$\hat{p}$ etc. evolve in time, the dynamics are more intuitive and familiar. A drawback of the Heisenberg picture is the inevitability of the transition rates and probabilities becoming very bulky when using higher-order operators. Reviewing the development of traditional quantum pictures becomes fruitful when we consider the Wei-Norman Ansatz for the time-evolution operator. We then see that the time-dependence moves into the Lie algebra parameters that give us four ODEs. This method allows easy access of transition amplitudes of any order *and* phase-space simultaneously. We begin this section by reviewing the dipole model in the Heisenberg picture as this is a great warm-up for the Lie Algebraic approach.

Heisenberg Picture

We begin applying the Heisenberg picture by defining a Heisenberg algebra as the set of complex elements $\{\hat{x},\hat{p},1\}$ being closed under commutation, i.e. $[\hat{x},\hat{p}]=i\hbar$ where $i\hbar$ is contained in the algebra. An oscillator driven by an external field $f(t)$ is then modeled by forming a boson algebra $\left\{\hat{a}^{\dagger},\hat{a},1\right\}$ with the linear combinations of the Heisenberg algebra basis elements $\hat{x}$ and $\hat{p}$

$$\hat{a}^{\dagger}=\sqrt{\frac{m\omega}{2\hbar}}\left(\hat{x}-\frac{i}{m\omega}\hat{p}\right)\text{ and }\hat{a}=\sqrt{\frac{m\omega}{2\hbar}}\left(\hat{x}+\frac{i}{m\omega}\hat{p}\right), \tag{2.6}$$

which satisfy the condition of an equal time commutation relation

$$\left[\hat{a}(t),\hat{a}^{\dagger}(t)\right]=1 \tag{2.7}$$

allowing a compact Hamiltonian expression

$$\hat{H}=\hbar\omega\left(\hat{a}^{\dagger}\hat{a}+\frac{1}{2}\right)+\hat{a}f(t)+\hat{a}^{\dagger}f^{*}(t). \tag{2.8}$$

Note the higher order term $\hat{a}^{\dagger}\hat{a}$ shows that $\hat{H}$ is not a part of the $\{\hat{x},\hat{p},1\}$ algebra. The dynamics that we are interested in are contained in the algebra, not the Hamiltonian. The equations-of-motion are found with the Heisenberg equation-of-motion for an observable. For $\hat{a}$ the equation-of-motion is

$$\frac{d\hat{a}(t)}{dt}+i\omega\hat{a}(t)=-\frac{i}{\hbar}f^{*}(t). \tag{2.9}$$

Notice that with the field turned off, the solution is simply $\hat{a}(t)=a_0e^{-i\omega t}$, just a phase that we multiply the initial operator with (analog to stationary states). Also, the time-dependent part becomes a driving term, an indirect connection to the distant charge in motion that created this local field. This is an inhomogeneous differential equation, which is easily solved by standard methods. For instance, it can be multiplied by the integrating factor $e^{i\omega t}$ and cast into the form

$$\frac{d}{dt}\left[\hat{a}(t)e^{i\omega t}\right]=-\frac{i}{\hbar}f^{*}(t)e^{i\omega t}, \tag{2.10}$$

where choosing $t_0=0$ we may easily integrate to produce the general solution

$$\hat{a}(t)=\hat{a}e^{-i\omega t}-\frac{i}{\hbar}\int_0^t e^{-i\omega(t-t')}f^{*}\left(t'\right)dt'. \tag{2.11}$$

With this and the solution for $\hat{a}^\dagger$, if we are given an explicit field we can now find phase-space dynamics with

$$\langle \hat{x} \rangle = \sqrt{\frac{1}{2m\omega}} \left(\langle \hat{a}(t) \rangle + \left\langle \hat{a}^\dagger(t) \right\rangle \right) \tag{2.12}$$

and

$$\langle \hat{p} \rangle = i\sqrt{\frac{m\omega}{2}} \left(\left\langle \hat{a}^\dagger(t) \right\rangle - \langle \hat{a}(t) \rangle \right). \tag{2.13}$$

For many systems this is sufficient. However, to consider transition amplitudes from an energy state $|n\rangle \to |m\rangle$ corresponding to the eigenstate of the number operator $\hat{N} = \hat{a}^\dagger \hat{a}$, a bulky calculation (2.14) is necessary,

$$\langle m | \left[\hbar\omega \left(\hat{a}^\dagger \hat{a} + \frac{1}{2} \right) + \hat{a} f(t) + \hat{a}^\dagger f^*(t) \right] |n\rangle . \tag{2.14}$$

The linear structure in the amplitudes would also occur when taking the time-evolution operator to be an exponential of the sum of operators. We will see how the Baker-Campbell-Hausdorff formula (Appendix C.5) and adding a dimension to our algebra will significantly simplify this.

2.3 Lie Algebraic Approach

We are now prepared to introduce the abstract algebraic approach in full detail. Introducing a closed Lie algebra with basis elements $\left\{ \hat{a}^\dagger, \hat{a}, \hat{N}, 1 \right\}$ we will solve the Schrödinger equation for the time-evolution operator $\hat{U}(t)$:

$$i\frac{d}{dt}\hat{U} = \hat{H}\hat{U}. \tag{2.15}$$

where we let $\hbar = 1$. We now take advantage of the Wei-Norman Ansatz [9]. The Wei Norman Ansatz consists in writing the evolution operator as a product of four exponentials each one corresponding to each of the elements of the basis of the Lie algebra. The operator in the exponent is multiplied by a commuting time-dependent factor in the following way:

$$\hat{U} = e^{\alpha_1 \hat{a}^\dagger} e^{\alpha_2 \hat{a}} e^{\alpha_3 \hat{N}} e^{\alpha_4}. \tag{2.16}$$

We apply the Wei-Norman Ansatz to both sides of (2.15) and invert the RHS Ansatz to get

$$i\left(\frac{d}{dt}e^{\alpha_1\hat{a}^\dagger}e^{\alpha_2\hat{a}}e^{\alpha_3\hat{N}}e^{\alpha_4}\right)e^{-\alpha_4}e^{-\alpha_3\hat{N}}e^{-\alpha_2\hat{a}}e^{-\alpha_1\hat{a}^\dagger}=\hat{H}. \tag{2.17}$$

Equating coefficients of the Lie algebra elements in (2.17) produces 4 differential equations for the time-dependent c-numbers $\alpha_1(t), \alpha_2(t)\alpha_3(t)$, and $\alpha_4(t)$. To massage the LHS of (2.17) into a form where the algebraic properties may be exploited we separate the exponential terms using the Baker-Hausdorf formula (Appendix B.5). We substitute in the specific Hamiltonian for an external dipole field given by (2.8) for the RHS of (2.17) bringing us to

$$\begin{aligned} &i\left(\dot{\alpha}_1-\dot{\alpha}_3\alpha_1\right)\hat{a}^\dagger+i\left(\dot{\alpha}_2+\dot{\alpha}_3\alpha_2\right)\hat{a}+i\left(\dot{\alpha}_3\right)\hat{N}+i\left(\dot{\alpha}_4-\dot{\alpha}_3\alpha_2\alpha_1-\dot{\alpha}_2\alpha_1\right) \\ &\qquad=\left(f\left(t\right)\right)\hat{a}^\dagger+\left(f\left(t\right)\right)\hat{a}+\left(\omega\right)\hat{N}+\left(\tfrac{1}{2}\omega\right). \end{aligned} \tag{2.18}$$

When we equate the coefficients of (2.18), we get 4 linear equations-of-motion

$$\dot{\alpha}_1+i\omega\alpha_1=-i\omega t \tag{2.19}$$

$$\dot{\alpha}_2-i\omega\alpha_2=f\left(t\right)+\omega\alpha_1 \tag{2.20}$$

$$\dot{\alpha}_4=f\left(t\right)-\omega\alpha_2 \tag{2.21}$$

$$\dot{\alpha}_3=-i\omega. \tag{2.22}$$

Now we may use a specific external field, i.e. $f\left(t\right)=\sqrt{\frac{E_0^2}{2m\omega}}\cos\omega_0 t$ and get the α solutions as explicit functions of time corresponding to the oscillator's dynamics.

Dipole Field Transitions

Finding the probabilities for the oscillator to gain quanta of energy from the field is the next step. Knowing the explicit forms of these Lie coefficients we can calculate persistence amplitudes,

$$\langle n|\hat{U}|n\rangle=\langle n|e^{\alpha_1\hat{a}^\dagger}e^{\alpha_2\hat{a}}e^{\alpha_3\hat{N}}e^{\alpha_4}|n\rangle \tag{2.23}$$

or time-dependent transition amplitudes

$$\langle n|\hat{U}|m\rangle=\langle n|e^{\alpha_1\hat{a}^\dagger}e^{\alpha_2\hat{a}}e^{\alpha_3\hat{N}}e^{\alpha_4}|m\rangle. \tag{2.24}$$

2.4 Results and Summary

We now take a look at some results of the dipole field model. In Figs. 2.1 through 2.5 we compare phase space trajectories to the cooresponding time-dependent transition probabilities. Fig. 2.1 shows two asymptotic states of a harmonically oscillating charge, seen as small and large circles, connected by a transient oscillation. Fig. 2.2 is the plot of an oscillator that receives a pulse of energy from the external field and then proceeds to oscillate at a greater amplitude. We start the quantum dynamics in a single ground state and show how higher order transitions grow in amplitude after the collision in Fig. 2.3. In Fig. 2.4 we turn the external field on at $t = 0$ and compare the plots of the field strength and the amplitude of the oscillator to see how they correspond in time.

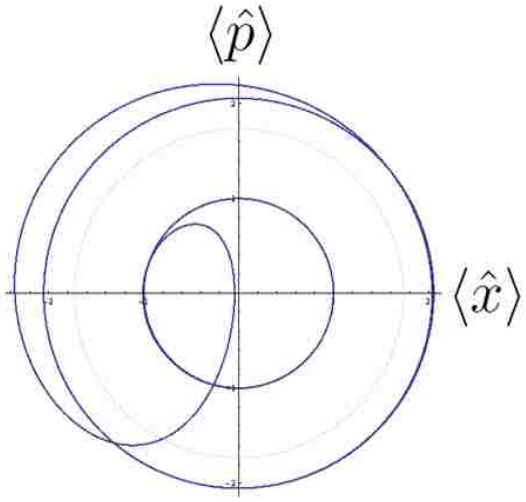

Figure 2.1 Phase-space trajectories for a harmonic oscillator absorbing energy from a pulse field. This plot shows two asymptotic states of a harmonically oscillating charge, seen as small and large circles, connected by a transient oscillation.

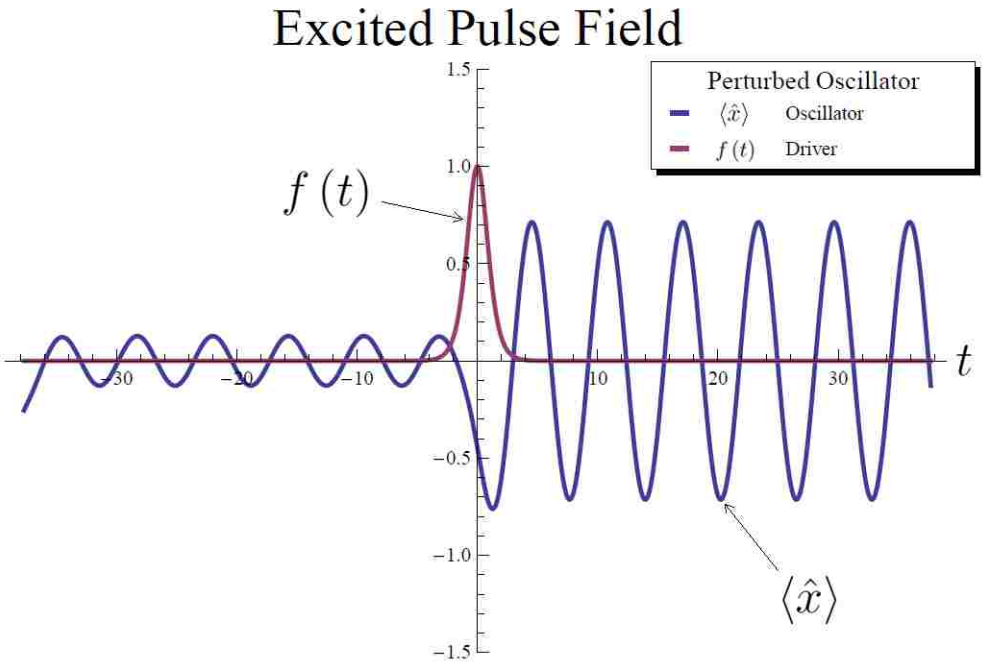

Figure 2.2 Time-dependence of the oscillator subject to an external field pulse. This is the plot of an oscillator that receives a pulse of energy from the external field and then proceeds to oscillate at a greater amplitude.

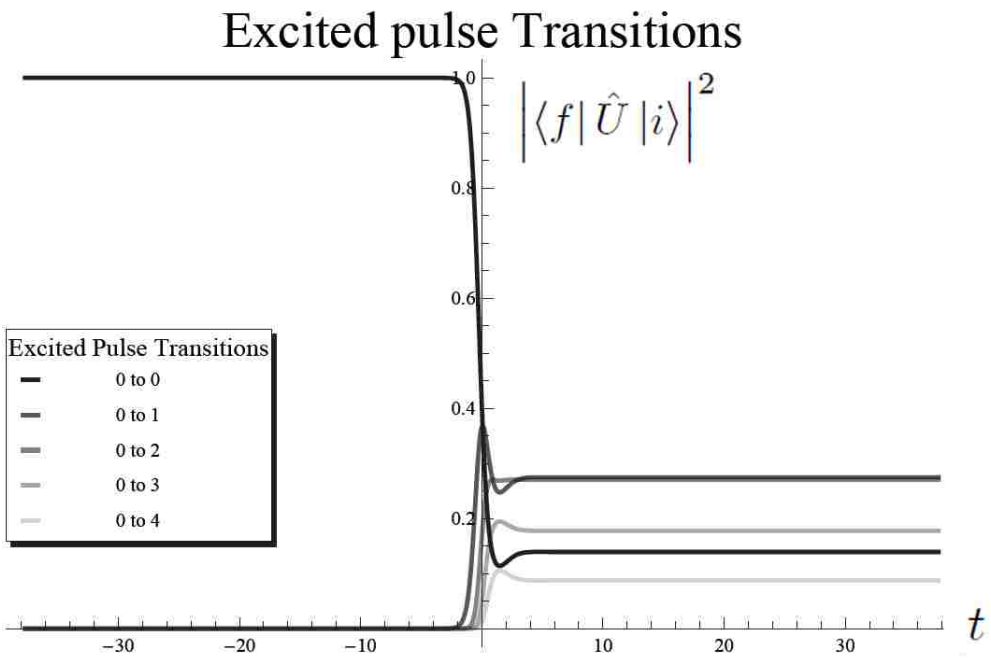

Figure 2.3 Quantum transition amplitudes of an oscillator initially in the single ground state (Appendix C.1).

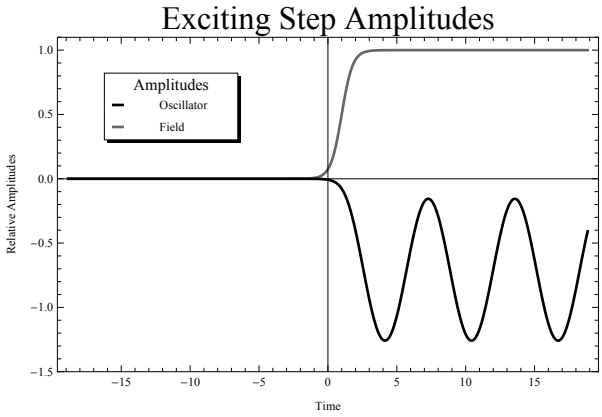

a)

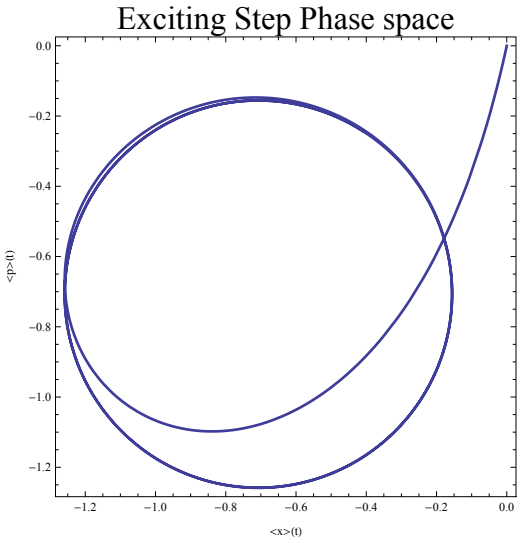

b)

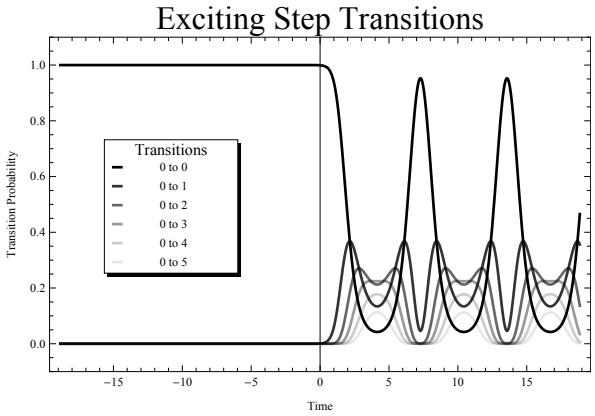

c)

Figure 2.4 External field turns on at $t = 0$ and leave it on. a) we see the plots of the field strength and the amplitude of the oscillator and how they correspond in time. b) is the phase-space plot of the exact same event. Notice that the initial expectation value for the oscillator is not oscillating (Appendix C.3). c) Transition probabilities for gound state to nearby low energy states.

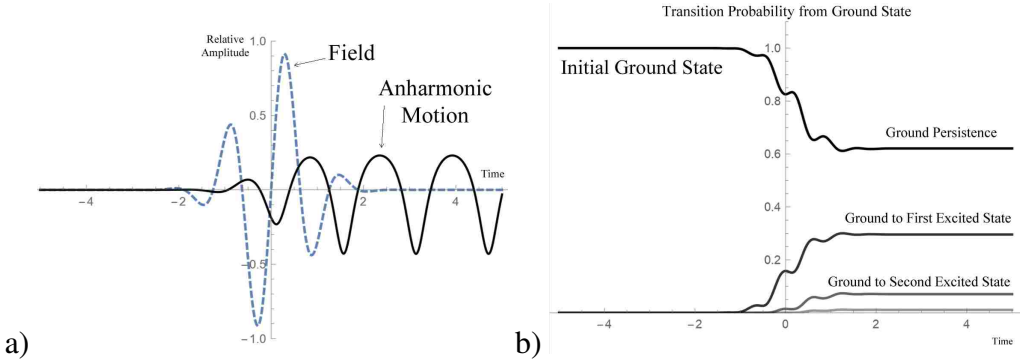

Figure 2.5 a) When we include the anharmonic potential in the calculations we can see the oscillator now has cusps as expected. Notice the external field $\left(\propto \sin(\omega t)e^{-t^2}\right)$ contains a frequency ω that can resonate with the oscillator. b) Transition amplitudes from ground to the first and second excited states throughout time as the charge oscillates in the external field. Note that when the field is turned off the phase relations are constant again unlike when the field is left on in Fig. 2.4 c).

In Fig. 2.5 we excite the anharmonic oscillator with a harmonic sinusoidal external field on resonance. When we rearrange the Schrödinger operator equation into (2.17) we can exploit the Wei-Norman Ansatz by equating Lie algebra coefficients. This produces the equations-of-motion from which both phase-space dynamics and transition probabilities are derived. When we solve the four differential equations for α_i we have enough information for state-to-state transition probabilities,

$$\langle n|\hat{U}|m\rangle = \langle n| e^{\alpha_1 \hat{a}^\dagger} e^{\alpha_2 \hat{a}} e^{\alpha_3 \hat{N}} e^{\alpha_4} |m\rangle \tag{2.25}$$

and phase-space dynamics with

$$\langle \hat{a} \rangle = \langle n|\hat{U}^{-1}\hat{a}\hat{U}|n\rangle \tag{2.26}$$

and

$$\left\langle \hat{a}^\dagger \right\rangle = \langle n|\hat{U}^{-1}\hat{a}^\dagger\hat{U}|n\rangle . \tag{2.27}$$

I chose the driven harmonic oscillator as an example because of its similarity to an inelastic molecular collision [10, 11]. In this chapter I introduced the important mathematical ideas needed

to apply the theory beyond a dipole field. In the following chapters I develop some relevant examples of molecular collisions.

Chapter 3

Inelastic Molecular Collisions

I now apply the algebraic quantum dynamic model discussed in Chapter 2 to inelastic molecular collisions. I focus on a collinear inelastic collision between a diatomic molecule and an atom. This is generally called the Landau-Teller model because it models the diatomic molecule as a harmonic oscillator with an exponential repulsion between the incoming atom and the closest atom of the molecule. My contribution is threefold: a) a Lie algebraic approach to study this model, b) the coupling between the translational and vibrational motions, solving all the equations simultaneously, and c) the time evolution of a thermal mixture of initial states.

The inelastic collision system behaves very similarly to the driven (atomic collision) quantum oscillator (vibrating molecule) but a new challenge arises since it is now a three-body problem. I begin tackling the problem by removing the center-of-mass motion for the whole system. I then note that the translation of the atom relative to the molecule is essentially classical in nature. I treat the vibrating molecule as an oscillating dimensionless reduced mass with quantized motion. This combination of classical and quantum degrees-of-freedom is what is meant by "semi-classical" in the title of this thesis.

My first contribution begins when I construct a Hamiltonian for this reduced system with Lie algebra elements and derive four quantum equations of motion. With the solutions loaded into the

time-evolution operator, I am able to plot the phase-space trajectory of the oscillator as it is excited from a ground state. I simultaneously plot transition probabilities from this ground state to any other state continuously throughout the excitation. I then iterate a single collision condition into a canonical ensemble. The plots show quantum dynamics of a bath of molecules leaving thermal equilibrium with the atoms.

My molecular collision calculations are performed non-perturbatively exploiting the algebraic properties of the system. In particular, I consider a model Hamiltonian with time as a parametric variable and where both the oscillator and the atomic interaction terms contain time-dependent coefficients. The operator part of the Hamiltonian is written in terms of elements of a Lie algebra. Given that the resulting algebra is closed under commutation, one can express the time-evolution operator $\hat{U}$ as a product of exponentials, each corresponding to a single generator of the algebra [9]. Within this scheme the time-dependence is concentrated in the commuting coefficients $\{\alpha_i\}$ appearing in the exponents, as will become evident in what follows. The differential equation fulfilled by the evolution operator $\hat{U}$ is replaced by a set of coupled ordinary differential equations for the α's that can be solved numerically. Armed with $\hat{U}$, one can easily obtain

(a) time-dependent transition probabilities between two of the oscillator states induced by the incoming atom

(b) the expectation value of the Heisenberg position and momentum operators

(c) a plot of the corresponding phase-space trajectory

In deriving the Hamiltonian I also make use of a shift in the oscillator frequency. I then allow the oscillator frequency to be dependent on the distance between the incoming atom and the diatomic molecule's center-of-mass. This is the result of a coupling between the classical equation for translation and the quantum equation for the oscillator. Previous work assumes a precalculated incoming classical trajectory for the atom [1].

In the results of this section, I develop these ideas into a working model and find the expressions

for the transition probabilities as a function of time, as well as the time-evolution of the average position and momentum. A temperature-dependent case of a Boltzmann distribution of initial conditions with single and mixed states is then discussed. The promise of this work lies in the fact that it is a unique combination of proven methods, most of which are already used by modern molecular collision theorists [1, 10, 14].

3.1 The Coordinates

Consider a simple collinear inelastic collision between a diatomic molecule and an atom. We set up the following coordinates [15] for the nuclei positions as in Fig. 3.1.

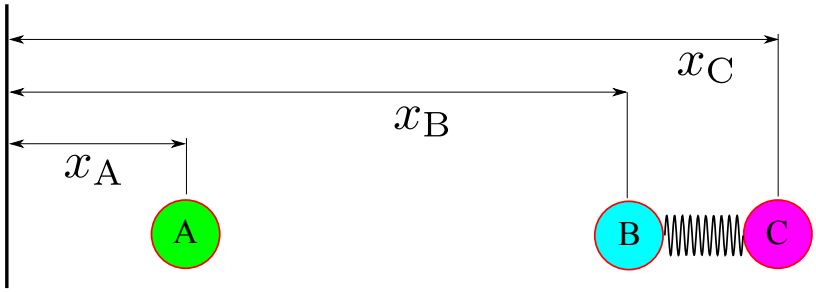

Figure 3.1 Initial coordinate system for a collinear triatomic system.

Classically the Hamiltonian for the Landau-Teller model would be

$$H_1 = \frac{p_A^2}{2m_A} + \frac{p_B^2}{2m_B} + \frac{p_C^2}{2m_C} + V_{BC}(x_B - x_C) + V_{AB}(x_A - x_B). \tag{3.1}$$

Here we take the B and C atoms to be bound and the interaction between C and A to be negligible. We may reduce the problem to two dimensions using the following Jacobi coordinates shown in Fig. 3.2.

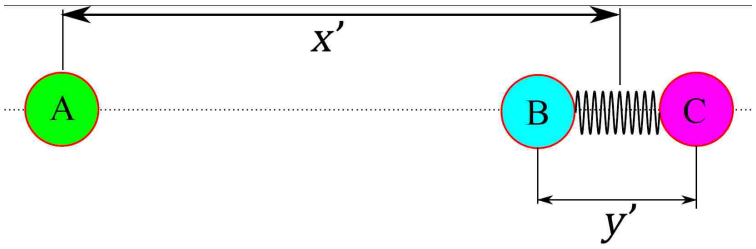

Figure 3.2 Coordinate system after the removal of the center-of-mass.

The coordinates in Fig. 3.2 are defined as follows: y' is the distance between the nuclei in the diatomic molecule. Take x' to be the distance between the A atom and the centers-of-mass of B and C. Consider X the distance of the whole system's center-of-mass to the origin. The explicit equations of transformation are

$$\begin{gathered} y' = x_{\mathrm{B}} - x_{\mathrm{C}}, \quad x' = x_{\mathrm{A}} - \frac{m_{\mathrm{B}}x_{\mathrm{B}}+m_{\mathrm{C}}x_{\mathrm{C}}}{m_{\mathrm{B}}+m_{\mathrm{C}}}, \quad X = \frac{m_{\mathrm{A}}x_{\mathrm{A}}+m_{\mathrm{B}}x_{\mathrm{B}}+m_{\mathrm{C}}x_{\mathrm{C}}}{m_{\mathrm{A}}+m_{\mathrm{B}}+m_{\mathrm{C}}} \\ \mu_{\mathrm{BC}} = \frac{m_{\mathrm{B}}m_{\mathrm{C}}}{m_{\mathrm{B}}+m_{\mathrm{C}}}, \quad \mu_{\mathrm{A,BC}} = \frac{m_{\mathrm{A}}(m_{\mathrm{B}}+m_{\mathrm{C}})}{m_{\mathrm{A}}+m_{\mathrm{B}}+m_{\mathrm{C}}} \end{gathered} . \tag{3.2}$$

Now when we transform the Hamiltonian, we can ignore the kinetic energy of the center-of-mass and get

$$H_2 = \frac{p_{y'}^2}{2\mu_{\mathrm{BC}}} + \frac{p_{x'}^2}{2\mu_{\mathrm{A,BC}}} + V_{\mathrm{BC}}\left(y'\right) + V_{\mathrm{AB}}\left(x' - \frac{\mu_{\mathrm{BC}}}{m_{\mathrm{B}}}y'\right). \tag{3.3}$$

3.2 The Landau-Teller Model

We now choose a simple potential and the appropriate transformation to dimensionless variables x and y. A potential appropriate for the harmonic motion of the diatomic system is given and then transformed into y:

$$V_{\mathrm{BC}}\left(y'\right) = \frac{1}{2}\mu_{\mathrm{BC}}\omega_0^2\left(y'-y_0\right)^2 = \frac{1}{2}\hbar\omega_0 y^2. \tag{3.4}$$

where ω_0 is the natural vibrational frequency of the diatomic molecule. Isolating the vibrational degree-of-freedom we get the dimensionless displacement

$$y = \sqrt{\frac{\omega_0\mu_{\mathrm{BC}}}{\hbar}}\left(y'-y_0\right). \tag{3.5}$$

For the potential representing the atom/molecule interaction it is essential to transform y' to y with

$$V_{\mathrm{AB}}\left(x' - \frac{\mu_{\mathrm{BC}}}{m_{\mathrm{B}}}y'\right) = \hbar\omega_0 V\left(x-y\right) = \hbar\omega_0 V_0 e^{-\beta(x-y)}. \tag{3.6}$$

where both V_0 and β are dimensionless parameters defining the atom-diatomic interaction. After making the change to relative dimensionless variables there appears a coupling between x and y. These momentum operators now refer to reduced mass particles 1 and 2 at positions away from their respective centers-of-mass like in Fig. 3.3.

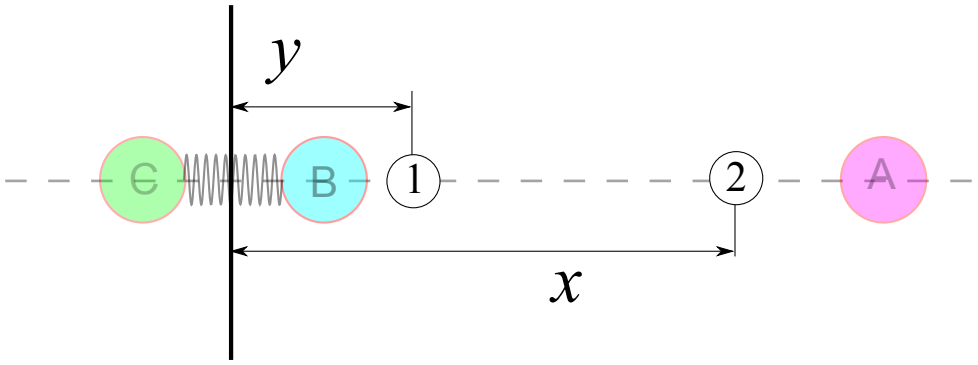

Figure 3.3 Final coordinate system of choice.

The easy route here is to avoid solving this wave-equation and break the coordinates up into classical and quantum degrees-of-freedom. The kinetic and potential energies are now:

$$\hat{T} = \frac{1}{2m}\hbar\omega_0 p_x^2 + \frac{1}{2}\hbar\omega_0\hat{p}_y^2 \tag{3.7}$$

and

$$\hat{V} = \hbar\omega_0\frac{1}{2}\hat{y}^2 + \hbar\omega_0 V_0 e^{-\beta(x-\hat{y})}. \tag{3.8}$$

Note m is now defined as a dimensionless mass used in the transformation: $\hat{p}_{x'} \rightarrow \sqrt{\frac{\mu_{\mathrm{A,BC}}\hbar\omega_0}{m}}\hat{p}_x$, or explicitly $m = \frac{m_{\mathrm{A}}m_{\mathrm{C}}}{m_{\mathrm{B}}(m_{\mathrm{A}}+m_{\mathrm{B}}+m_{\mathrm{C}})}$. Now divide out by $\hbar\omega_0$ and transform into new scaled energy units to get our final workable semi-classical Hamiltonian of

$$\hat{H}_{\mathrm{sc}} = \frac{1}{2m}p_x^2 + \frac{1}{2}\hat{p}_y^2 + \frac{1}{2}\hat{y}^2 + V_0 e^{-\beta(x-\hat{y})}. \tag{3.9}$$

At this point we interpret the x coordinate to be a classical relative translation of the atom and molecule while $\hat{y}$ is a displacement operator for the quantum vibration of the diatomic molecule. Our classical equation is

$$m\frac{d^2x}{dt^2} = -\partial_x V_0 e^{-\beta x} e^{\beta \langle \hat{y} \rangle (t)} = \beta V_0 e^{-\beta x} e^{\beta \langle \hat{y} \rangle (t)}. \tag{3.10}$$

where $\langle \hat{y} \rangle (t)$ is the time-dependent expectation value of the vibrational displacement operator $\hat{y}$. While the quantum equation is taken to be

$$i\frac{d}{dt}\hat{U}(t) = \hat{H}\hat{U}(t) \tag{3.11}$$

where the LHS has $\hbar\omega_0$ divided out and applies a variable redefinition of $t = t'\omega_0$ giving us our workable *Quantum* Hamiltonian

$$\hat{H}_{\mathrm{q}} = \frac{1}{2}\hat{p}_y^2 + \frac{1}{2}\hat{y}^2 + V_0 e^{-\beta x} e^{\beta \hat{y}}. \tag{3.12}$$

Notice that the only mass left after all the transformations is associated to the translational degree of freedom. The quantum Hamiltonian (3.12) contains no explicit mass at all. The classical variable x is updated numerically from the classical equation-of-motion each step. Given that the motion along the vibrational coordinate y is restricted, some approximations become appropriate at this point. First, expansion of the exponential repulsive term

$$V_0 e^{-\beta x} e^{\beta \hat{y}} \approx V_0 e^{-\beta x}\left(1 + \beta\hat{y} + \frac{1}{2}\beta^2\hat{y}^2 + \ldots\right) \tag{3.13}$$

gives us the truncated quantum Hamiltonian,

$$\hat{H}_{\mathrm{q}} = \frac{1}{2}\hat{p}_y^2 + \frac{1}{2}\hat{y}^2\left(1 + \beta^2 V_0 e^{-\beta x}\right) + V_0 e^{-\beta x} + \beta\hat{y}V_0 e^{-\beta x}. \tag{3.14}$$

Now the quadratic term in y can be redefined with a new angular frequency of

$$\Omega^2(x(t)) = 1 + \beta^2 V_0 e^{-\beta x}, \tag{3.15}$$

giving us

$$\hat{H}_{\mathrm{q}} = \frac{1}{2}\hat{p}_y^2 + \frac{1}{2}\Omega^2\hat{y}^2 + V_0 e^{-\beta x} + \beta\hat{y}V_0 e^{-\beta x}. \tag{3.16}$$

The Landau-Teller Hamiltonian (3.16) corresponding to the quantum harmonic oscillator has the following features: a) it is effectively time-dependent through the dependence of the classical translational degree-of-freedom $x(t)$; b) it involves an x dependent dynamic angular frequency $\Omega(x(t))$ which adapts to the ongoing translational motion; c) it includes an x dependent driving term due to the atom-diatomic interaction.

Note the coupling of the molecule vibration $\hat{y}$ to the relative translation of the colliding species x in the last term of the Hamiltonian. In previous work [2, 16], this interaction term assumes a precalculated trajectory (external driving field) such as $\text{sech}^2(t)$.

It is appropriate to utilize an algebraic approach in the construction of the system dynamics at this point. We start with a Lie algebra made of a set of the elements, $\left\{\hat{a},\hat{a}^\dagger,\hat{N},1\right\}$, that is closed under commutation relations,

$$\left[\hat{a},\hat{a}^\dagger\right]=1 \qquad \left[\hat{a},\hat{N}\right]=\hat{a} \qquad \text{and} \qquad \left[\hat{a}^\dagger,\hat{N}\right]=-\hat{a}^\dagger. \tag{3.17}$$

With this particular Lie algebra it is of interest that (3.16) be rewritten in terms of the boson operators $\hat{a}$ and $\hat{a}^\dagger$. This is done with the ladder operator/phase-space relations in (3.18).

$$\hat{y}=\sqrt{\frac{1}{2\Omega}}\left(\hat{a}^\dagger+\hat{a}\right) \quad \text{and} \quad \hat{p}_y=i\sqrt{\frac{\Omega}{2}}\left(\hat{a}^\dagger-\hat{a}\right) \tag{3.18}$$

The subtitution produces the desired quantum Hamiltonian:

$$\hat{H}=\frac{1}{2}\left[i\sqrt{\frac{\Omega}{2}}\left(\hat{a}^\dagger-\hat{a}\right)\right]^2+\frac{1}{2}\Omega^2\left[\sqrt{\frac{1}{2\Omega}}\left(\hat{a}^\dagger+\hat{a}\right)\right]^2+V_0e^{-\beta x}+\beta\sqrt{\frac{1}{2\Omega}}\left(\hat{a}^\dagger+\hat{a}\right)V_0e^{-\beta x}. \tag{3.19}$$

The effective frequency of oscillation now takes the functional form of

$$\Omega(x)=\sqrt{1+\beta^2V_0e^{-\beta x}}, \tag{3.20}$$

which introduces a new quadratic term in $\hat{y}$ redefining the angular frequency.

Equations of Motion

The time dependence for $\hat{y}$ moves into the four Lie algebra parameters α_i. We use the Ansatz of choice [9] for the quantum equation:

$$\hat{U}(t) = e^{\alpha_1 \hat{a}^\dagger} e^{\alpha_2 \hat{a}} e^{\alpha_3 \hat{N}} e^{\alpha_4}. \tag{3.21}$$

This defines the general quantum solution. Inverting the Ansatz in (3.21) isolates the Hamiltonian. In our case it is rewritten in linear and quadratic terms of boson algebra elements as

$$\hat{H} = \left(V_0 e^{-\beta x} + \frac{\Omega}{2}\right) + \left(\beta\sqrt{\frac{1}{2\Omega}} V_0 e^{-\beta x}\right)\hat{a} + \left(\beta\sqrt{\frac{1}{2\Omega}} V_0 e^{-\beta x}\right)\hat{a}^\dagger + (\Omega)\,\hat{a}^\dagger\hat{a}. \tag{3.22}$$

Note: $\hat{a}\hat{a}^\dagger = 1 + \hat{N}$. The challenging part begins as we use commutation relations (Appendix C.4) and a few other mathematical rearrangements bringing us to the quintessential Schrödinger equation

$$\hat{H} = (i\dot{\alpha}_3)\,\hat{a}^\dagger\hat{a} + (i\dot{\alpha}_1 - i\dot{\alpha}_3\alpha_1)\,\hat{a}^\dagger + (i\dot{\alpha}_2 + i\dot{\alpha}_3\alpha_2)\,\hat{a} + (i\dot{\alpha}_4 - i\dot{\alpha}_2\alpha_1 - i\dot{\alpha}_3\alpha_2\alpha_1)\,1. \tag{3.23}$$

This is a standard result using the Wei-Norman Ansatz for the four dimensional Lie algebra $\rightarrow \left\{\hat{a}, \hat{a}^\dagger, \hat{N}, 1\right\}$ (Appendix D.1). It is now possible to equate the Lie algebra coefficients using the above Hamiltonian and get the following coupled equations of motion.

$$\begin{aligned}
\ddot{x}(t) =& \frac{1}{m}\beta V_0 e^{-\beta x} e^{\beta\langle\hat{y}\rangle(t)} \\
\dot{\alpha}_1 =& -i\beta\sqrt{\frac{1}{2\Omega}} V_0 e^{-\beta x} + \dot{\alpha}_3\alpha_1 \\
\dot{\alpha}_2 =& -i\beta\sqrt{\frac{1}{2\Omega}} V_0 e^{-\beta x} - \dot{\alpha}_3\alpha_2 \\
\dot{\alpha}_3 =& -i\sqrt{1 + \beta^2 V_0 e^{-\beta x}} \\
\dot{\alpha}_4 =& -iV_0 e^{-\beta x} - i\frac{\Omega}{2} + \dot{\alpha}_2\alpha_1 + \dot{\alpha}_3\alpha_2\alpha_1
\end{aligned} \tag{3.24}$$

3.3 Results and Summary

Calculations with the current formulation are given when the time-evolution operator is found. We can compare the collinear trajectories and phase-space to see the energy transfer details and trajectory asymmetries by using the time-dependent expectation value for the quantum motion. Time-dependent probability of transition between arbitrary states is also readily available when the evolution operator is found. We show an example of this inelastic collision model in Fig. 3.4. Notice the asymmetry in the trajectory on the left as this is much more accurate than an uncoupled approach [2].

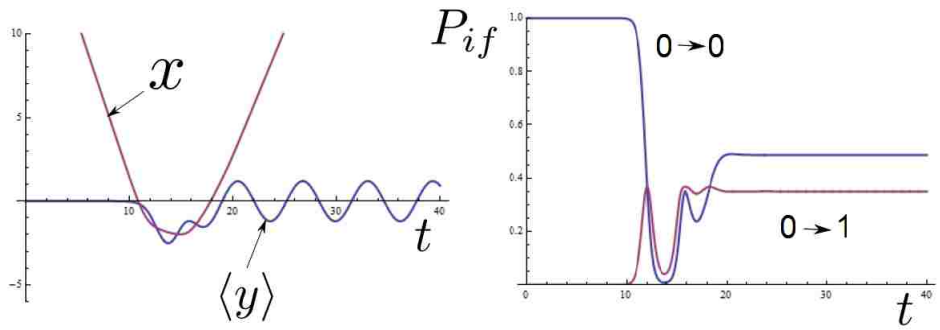

Figure 3.4 Here we have plotted the collinear trajectories as a function of time on the left and the time-dependent function $\left|\langle f|\hat{U}(t)|i\rangle\right|^2$ for $i=0$, and $f=0,1$ on the right. Notice the asymmetry in the trajectory on the left as this is much more accurate than an uncoupled approach [2]. In this case we used a single initial state (Appendix C.2) which is apparent in the initial transition probabilities for the ground and first excited states as well.

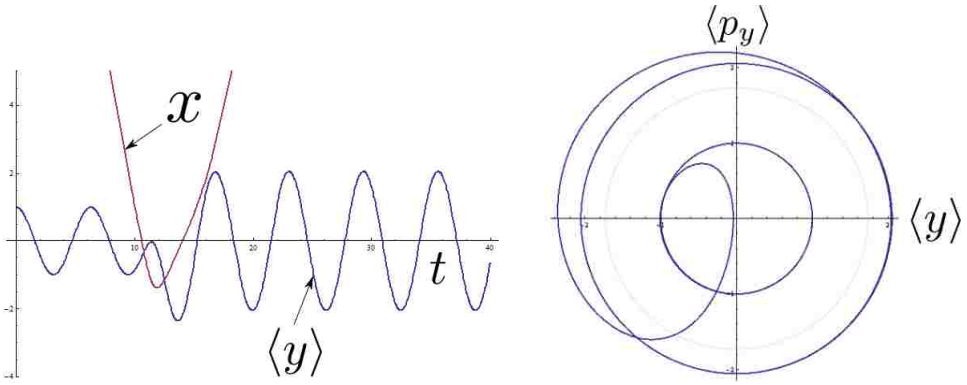

Figure 3.5 Another interesting initial condition is a linear combination of time-dependent states (Appendix C.3). This is seen in the fact that the expectation value of the position is not zero as would be in the previous case for an initial single state (Appendix C.1). To the right is the expectation value of phase-space for the harmonic oscillator corresponding to the collision this same collision.

Another interesting initial condition is a linear combination of time-dependent states shown in Fig. 3.5. This is seen in the fact that the expectation value of the position is not zero as would be in the previous case for an initial single state (Appendix C.1). To the right is the expectation value of phase-space for the harmonic oscillator corresponding to the collision this same collision. Figures 3.6-3.8 shows the probability of the single state oscillator to be found in the neighboring states after the collision can be seen as a dynamical landscape.

If we now analyze a canonical ensemble of oscillators before and after the collision we make use of a time-dependent probability of each oscillator state as

$$P_{if} = \left|\langle f|\,\hat{U}\rho_i\hat{U}^{-1}\,|f\rangle\right|^2 \frac{e^{-\beta E_i}}{Z}. \tag{3.25}$$

Plots in Figs. 3.6-3.8 are the distribution of states for a single state initial harmonic oscillator at temperature 50K. The initial state is seen as a spike. Notice the higher probability for the immediately neighboring states.

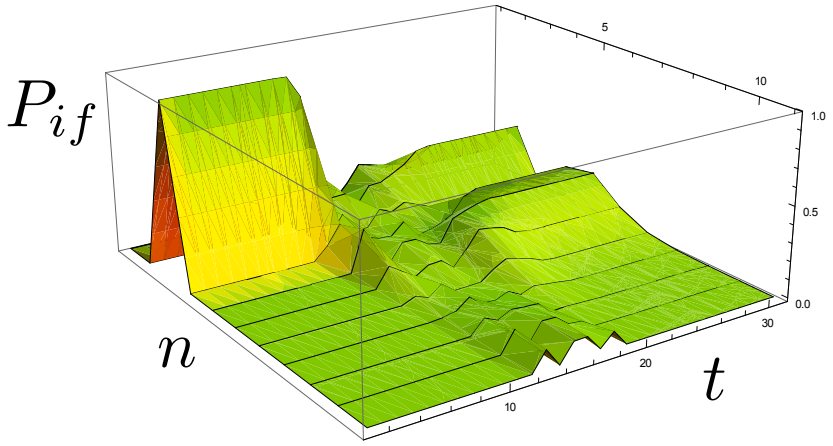

Figure 3.6 This is the time-dependence of the transition probability for the initial single state of $n = 2$ quanta. Notice during the collision the distribution is highly dispersed and messy. After the collision the diatomic molecule has high probability to move to the immediately neighboring states. This is not always the case, for some initial velocities the initial spike comes right back after the collision which refers to more adiabatic conditions.

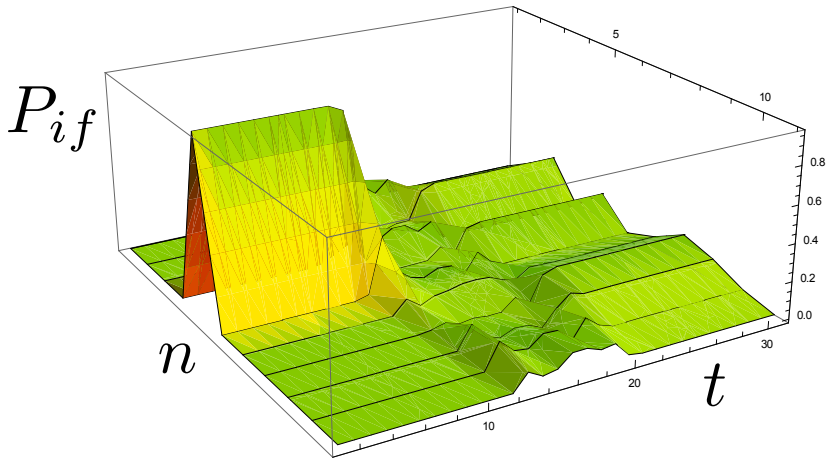

Figure 3.7 This is the time dependence of the transition probability for the in ital single state of $n = 4$ quanta. This time just after the collision the diatomic molecule has equal probability to move to the immediately neighboring states as well as remain in the initial state.

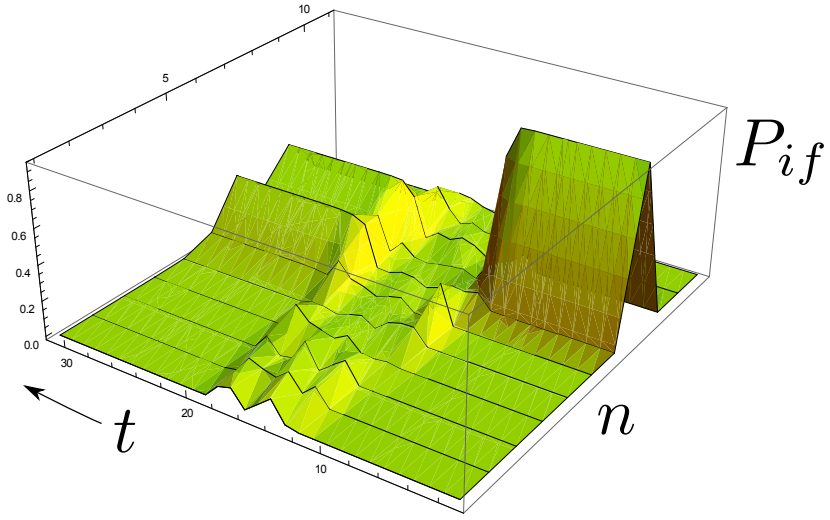

Figure 3.8 This is the time dependence of the transition probability for the initial state of $n = 7$ quanta where the plot has been rotated for a different perspective.

The Lie algebraic model has been shown to be a powerful formulation in inelastic molecular collision modeling. Finding the time-evolution operator produces all the information we need for both average phase-space and transitions of vibrationally excited diatomic molecules.

The Schrödinger equation in the form

$$i\left(\frac{d}{dt}\hat{U}\right)\hat{U}^{-1} = \hat{H}$$

has been shown to be a generalized tool one can tailor to a specific system. Time-resolved, infinite order transition probability calculations are a powerful result of the operator approach. We are now able to see details in the transition probabilities continuously through the whole collision. This work did not assume precalculated incoming atomic trajectories seen in previous work [1]. The model couples the atomic motion to the molecule's vibration producing assymetric collision trajectories. The next step is to build upon this method for the reactive case.

Chapter 4

Reactive Molecular Collisions

In this chapter the collinear reactive molecular collision is developed. The same reduced mass coordinate system used in the inelastic collision model now applies to both sides of the (Appendix B.5). I remove the centers-of-mass and use a natural reaction coordinate system that smoothly connects the reactant configuration to the product configuration. I take the translation along the reaction coordinate to be classical but I quantize the transverse coordinate since it will contain bound motion.

My contribution comes from constructing a reactive collision Hamiltonian with the same Lie algebra approach I used in the inelastic collision model. I start with a harmonic oscillator in the transverse direction and then move to the more realistic Morse potential where a mean field is applied. After the working model is developed I explore resonances in the trajectories and population inversion of the transition probabilities. I exploit the readily available state-to-state calculations by applying the model to atomic collisions with an initial Boltzmann distribution of molecular vibrational energies. I then discuss how the algebraic model reveals/resolves quantum dynamic details around the $A + BC \rightarrow AB + C$ reaction transition state. To highlight what my research adds to the field I start with a brief historical background of theoretical reaction dynamics relevant to my work.

4.1 Brief Reactive Collision Theory Background

In the first exact quantum mechanical inelastic collision calculations [15], a set of reduced-mass and mass-scaled Cartesian coordinates were used. Others were able to modify the potentials while still using these coordinates thereby making them a standard [3, 17].

In the pure quantum mechanical approach it was standard to separate the dynamics into two Hamiltonians, one for the reactant side and one for the product side [2]. This allowed asymptotic boundary conditions for reactive scattering, though two problems emerged. The normal inelastic approach by expansion in the reactant states led to heavy coupling between highly excited channels. At the same time, a mixed expansion in reactant and product states raises orthogonality issues and over-completeness in the basis set [14]. Finite difference methods were able handle these issues but tended to obscure the physical origin of the results. It wasn't until 1966 [18] that a curvilinear coordinate system[1] for reactive scattering was developed. Semi-classical methods are more intuitive in this natural coordinate system. The reaction coordinate, which represents the relative position of the colliding species, can now be treated classically. Only the coordinates perpendicular to the reaction coordinate need quantization.

A set of "normal coordinates" different from the natural ones were later introduced [19]. Interestingly, no articles cite these normal coordinates. The purpose of these "normal coordinates" was to gain a more intuitive understanding of the reaction by following the actual positions of the atoms, which the natural coordinates do not do. In most cases it is the transition probabilities that are needed and not the atomic motion anyway, and transition probabilities are independent of the coordinate system used. Although intuition of the exact motion of the masses is limited using natural coordinates, the transition probabilities are considered paramount as they may be compared to femtochemistry experiments.

[1] Appendix D.2

4.2 The Reactive Collision using Lie Algebra

Reactive or rearrangement processes differ from inelastic events by the appearance of new molecular species with different masses and different coordinate systems for these new molecules. It is the change in coordinate system which presents the most severe theoretical challenge. Mathematical transformations to the two axes R_{AB} and R_{BC} used in Fig. B.7 of the Appendix are needed to make this simulation quantitatively valid. The result of these operations is that the two new axes X and Y become skewed at an angle β relative to each other in a new mass-skewed coordinate system [20] seen in Fig. 4.1.

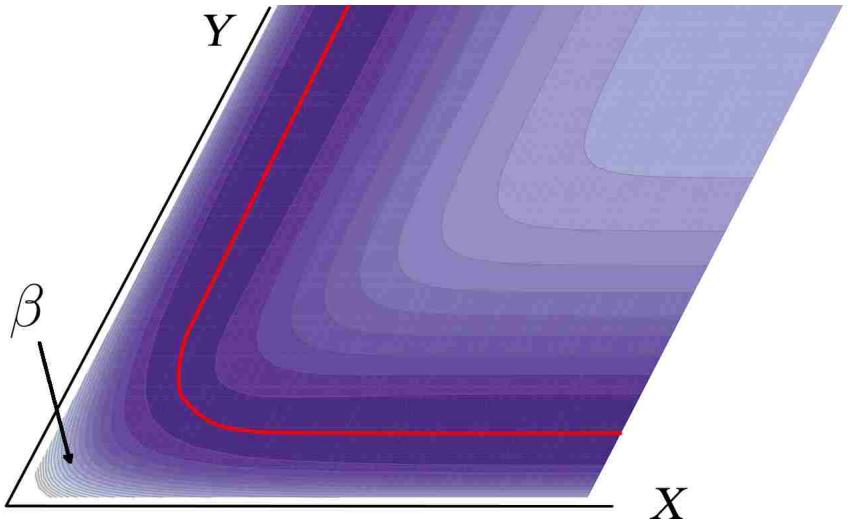

Figure 4.1 The skewed potential energy surface showing the minimum energy pathway defining the reaction coordinate

Highly skewed axes can have a dramatic effect on the reaction dynamics. In cases where the transition state is closer the product channel (a "late" transition state), which would normally channel energy into translation on a less unskewed surface, produces considerable vibrational excitation. Appendix D.2 shows a derivation of natural coordinates where this angle emerges.

We now describe our reactive collision model. Fig. 4.2 shows the important steps we took to develop the skewed reaction coordinate system needed for the model.

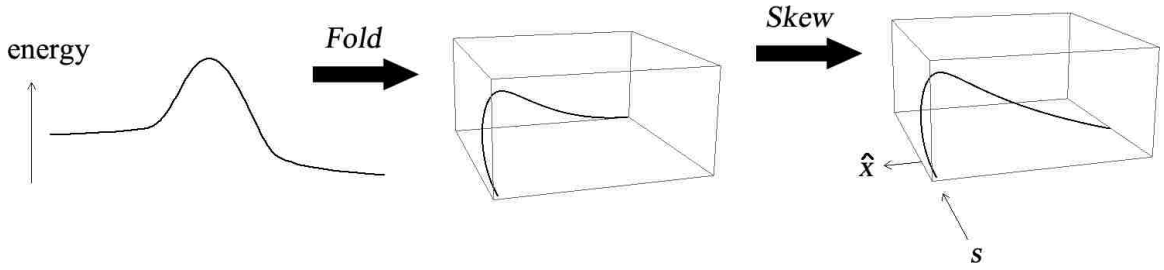

Figure 4.2 The development of the skewed reaction coordinate.

It is the reduced mass of all three atoms that is "sliding around on the potential energy surface". This transformation forces us into the skewed scheme. In the far right image of Fig. 4.2 we see two coordinates defined. The translational coordinate s is taken to be classical while the transverse motion, $\hat{x}$, is quantized. Since we are working with a semi-classical model we keep the hats on the quantum variables and take the hats off the classical variables. From M.S. Child's work in reactive scattering [14] we begin with the purely quantum Hamiltonian given in (4.1).

$$\hat{H} = -\frac{1}{2m}\left[\frac{\partial^2}{\partial \hat{x}^2} + \frac{\kappa^2}{4\eta^2}\right] + \hat{V}(s,\hat{x}), \tag{4.1}$$

where $\kappa(s)$ is the curvature of the "fold" seen in Fig. 4.2 and η is a function of κ and $\hat{x}$. Details to the derivation of this form are in Appendix D.2. An important feature to this expression is the coupling of the translational coordinate s and the transverse coordinate $\hat{x}$ in the "centrifugal term" $\kappa^2/4\eta^2$ because $\eta = 1 + \kappa(s)\hat{x}$. The word centrifugal is used here because of the term's strong effect on "pushing" the reaction away from the reaction coordinate as it crosses over the activated complex or saddle point. Our chosen potential and curvature functions for the reactive collision calculation are defined as

$$\hat{V}_{\mathrm{q}}(\hat{x}) = \frac{1}{2}m\omega(s)^2\hat{x}^2 \quad \text{and} \quad \kappa(s) = e^{-s^2}. \tag{4.2}$$

Notice the oscillator's frequency of transverse oscillation ω is a function of the reaction coordinate s. This means that the shape of the transverse oscillator adapts to the shape of the energy

surface as we evolve along the reaction coordinate. The Hamiltonian is now expressed as

$$\hat{H} = -\frac{1}{2m}\frac{\partial^2}{\partial \hat{x}^2} - \frac{e^{-2s^2}}{8m\left(1+e^{-s^2}\hat{x}\right)^2} + \frac{1}{2}m\omega(s)^2\hat{x}^2. \tag{4.3}$$

We begin our approximations with an expansion of the denominator resulting in

$$\approx -\frac{1}{2m}\frac{\partial^2}{\partial \hat{x}^2} + \frac{1}{2}m\omega(s)^2\hat{x}^2 - \frac{e^{-2s^2}}{8m}\left(1-2e^{-s^2}\hat{x}+3e^{-2s^2}\hat{x}^2\right). \tag{4.4}$$

Redefining the harmonic oscillator frequency as

$$\Omega^2(s) = \omega(s)^2 - \frac{3}{4m^2}e^{-4s^2} \tag{4.5}$$

creates the Hamiltonian of choice:

$$\hat{H} = -\frac{1}{2m}\frac{\partial^2}{\partial \hat{x}^2} + \frac{1}{2}m\Omega^2(s)\hat{x}^2 - \frac{e^{-2s^2}}{8m}\left(1-2e^{-s^2}\hat{x}\right). \tag{4.6}$$

This Hamiltonian represents a parametric harmonic oscillator with driving term on the far right. We now apply the Lie algebra method using the 4-dimensional algebra: $\left\{\hat{N},\hat{a},\hat{a}^\dagger,1\right\}$. Using the ladder operator/position-momentum relations, we explicitly rearrange the Hamiltonian to isolate the coefficients of the Lie Algebra elements:

$$\hat{H} = \Omega(s)\hat{N} + \left(\frac{e^{-s^2}}{4m}\sqrt{\frac{\Omega(s)}{2m}}\right)\hat{a}^\dagger + \left(\frac{e^{-s^2}}{4m}\sqrt{\frac{\Omega(s)}{2m}}\right)\hat{a} + \left(\frac{\Omega(s)}{2} - \frac{e^{-2s^2}}{8m}\right). \tag{4.7}$$

To equate it to the standard Lie algebra coefficients, we compare each side of

$$\hat{H} = i\dot{\alpha}_3\hat{N} + (i\dot{\alpha}_1 - i\dot{\alpha}_3\alpha_1)\hat{a}^\dagger + (i\dot{\alpha}_2 + i\dot{\alpha}_3\alpha_2)\hat{a} + (i\dot{\alpha}_4 - i\dot{\alpha}_2\alpha_1 - i\dot{\alpha}_3\alpha_2\alpha_1). \tag{4.8}$$

where the RHS comes from (3.23) and has been verified by symbolic manipulation in a Mathematica program (Appendix A.4 and C.5). Explicitly, the whole equation is:

$$\begin{aligned}&\Omega(s)\hat{N} + \left(\frac{e^{-s^2}}{4m}\sqrt{\tfrac{\Omega(s)}{2m}}\right)\hat{a}^\dagger + \left(\frac{e^{-s^2}}{4m}\sqrt{\tfrac{\Omega(s)}{2m}}\right)\hat{a} + \left(\frac{\Omega(s)}{2} - \frac{e^{-2s^2}}{8m}\right)1 \\ &= i\dot{\alpha}_3\hat{N} + (i\dot{\alpha}_1 - i\dot{\alpha}_3\alpha_1)\hat{a}^\dagger + (i\dot{\alpha}_2 + i\dot{\alpha}_3\alpha_2)\hat{a} + (i\dot{\alpha}_4 - i\dot{\alpha}_2\alpha_1 - i\dot{\alpha}_3\alpha_2\alpha_1),\end{aligned} \tag{4.9}$$

where the coeffiecient are in parentheses in fron of each element of the Lie Algebra. This produces the system of differential equations for the Lie algebra parameters,

$$\begin{aligned}
\dot{\alpha}_1 &= -i\frac{e^{-s^2}}{4m}\sqrt{\frac{\Omega(s)}{2m}} - i\Omega(s)\,\alpha_1 \\
\dot{\alpha}_2 &= -i\frac{e^{-s^2}}{4m}\sqrt{\frac{\Omega(s)}{2m}} + i\Omega(s)\,\alpha_2 \\
\dot{\alpha}_3 &= -i\Omega(s) \\
\dot{\alpha}_4 &= \dot{\alpha}_2\alpha_1 + \dot{\alpha}_3\alpha_2\alpha_1 - i\frac{\Omega(s)}{2} + i\frac{e^{-2s^2}}{8m}.
\end{aligned} \tag{4.10}$$

4.3 Including Anharmonic Molecular Vibrations

To complete our model we require a potential for the transverse coordinate that will result in more realistic, anharmonic behavior [21]. There also must be a chance for complete dissociation. The chosen potential and curvature functions for a more realistic scenario are defined as

$$\hat{V}(x) = V_0\left(1-e^{-\beta\hat{x}}\right)^2 \quad \text{and} \quad \kappa(s) = e^{-s^2}.$$

Plugging these into (4.1) we get,

$$\hat{H} = -\frac{1}{2m}\frac{\partial^2}{\partial\hat{x}^2} - \frac{e^{-2s^2}}{8m\left(1+e^{-s^2}\hat{x}\right)^2} + V_0\left(1-e^{-\beta\hat{x}}\right)^2. \tag{4.11}$$

Expanding the denominator and the Morse term (Appendix B.2), then redefining the harmonic oscillator frequency like we did in (4.5) we get

$$\hat{H} \approx -\frac{1}{2m}\frac{\partial^2}{\partial x^2} + \frac{1}{2}m\Omega^2\hat{x}^2 - \frac{e^{-2s^2}}{8m}\left(1-2e^{-s^2}\hat{x}\right). \tag{4.12}$$

We move to the Lie algebra representation [22] using the position/ladder operator relations and get:

$$\hat{H} = \Omega(s)\left(\hat{N}\right) + \left(\frac{e^{-s^2}}{4m}\sqrt{\frac{\Omega(s)}{2m}}\right)\hat{a}^\dagger + \left(\frac{e^{-s^2}}{4m}\sqrt{\frac{\Omega(s)}{2m}}\right)\hat{a} + \left(\frac{\Omega(s)}{2} - \frac{e^{-2s^2}}{8m}\right).$$

To derive the equations of motion we equate this Hamiltonian to the standard Lie algebra coefficients derived in Appendix D.1

$$\hat{H} = (i\dot{\alpha}_3)\hat{N} + (i\dot{\alpha}_1 - i\dot{\alpha}_3\alpha_1)\hat{a}^\dagger + (i\dot{\alpha}_2 + i\dot{\alpha}_3\alpha_2)\hat{a} + (i\dot{\alpha}_4 - i\dot{\alpha}_2\alpha_1 - i\dot{\alpha}_3\alpha_2\alpha_1)1. \tag{4.13}$$

Here are the equations of motion:

$$\begin{aligned}
\dot{\alpha}_1 =& \Omega(s)\alpha_1 - i\frac{e^{-s^2}}{4m}\sqrt{\frac{\Omega(s)}{2m}} \\
\dot{\alpha}_2 =& \Omega(s)\alpha_1 - i\frac{e^{-s^2}}{4m}\sqrt{\frac{\Omega(s)}{2m}} \\
\dot{\alpha}_3 =& -i\Omega(s) \\
\dot{\alpha}_4 =& \left(\Omega(s)\alpha_1 - i\frac{e^{-s^2}}{4m}\sqrt{\frac{\Omega(s)}{2m}}\right)\alpha_1 + \Omega(s)\alpha_2\alpha_1 - i\frac{\Omega(s)}{2} + i\frac{e^{-2s^2}}{8m}.
\end{aligned} \tag{4.14}$$

The solution to this system may then be used in the Wei-Norman ansatz to plot quantum dynamics of the reactive collision.

Mean-Field Approach

When we use the Morse potential it is inevitable that we end up with an $\hat{N}^2$ term. Rather than using a larger algebra to include this term we may construct a mean field Hamiltonian [8] starting with

$$\hat{H} = -\frac{1}{2m}\frac{\partial^2}{\partial\hat{x}^2} - \frac{\kappa^2}{8m(1+\kappa\hat{x})^2} + \hat{V}(s,\hat{x}). \tag{4.15}$$

We expand the denominator and the Morse term and redefine the oscillating frequency using

$$\frac{1}{2}m\omega^2 = D_0\alpha^2 - 3\frac{\kappa^4}{8m} \tag{4.16}$$

and

$$\omega(s) = \sqrt{\frac{2}{m}\left(D_0\alpha^2 - 3\frac{\kappa^4}{8m}\right)}. \tag{4.17}$$

One way to apply a mean field here is to consider the coefficient for the $\hat{N}^2$ term in a general Morse spectrum. Direct comparison of the current Hamiltonian with the standard Morse potential eigenvalues [23] via mean field gives us:

$$\hat{H} = \omega(s)\left(\hat{N}+\frac{1}{2}\right) - \chi\left(\hat{N}+\frac{1}{2}\right)^2 + \frac{\kappa^3}{4m}\hat{x} + V_0 e^{-\gamma s^2} - \frac{\kappa^2}{8m}. \tag{4.18}$$

Then we move to the Lie algebra representation using the position/ladder operator relation,

$$\hat{H} = \omega(s)\left(\hat{N}+\frac{1}{2}\right) - \chi\left(\hat{N}+\frac{1}{2}\right)^2 + \frac{\kappa^3}{4m}\sqrt{\frac{1}{2m\omega(s)}}\left(\hat{a}^\dagger+\hat{a}\right) + V_0 e^{-\gamma s^2} - \frac{\kappa^2}{8m}. \tag{4.19}$$

We now want to compare two different mean field approximations: The first method using mean field theory is to let $\hat{N} \to \langle \hat{N} \rangle$ and absorb the term into the harmonic oscillator frequency.

$$\hat{H}_{\mathrm{m}} = \Omega(s)\left(\hat{N}+\frac{1}{2}\right) + \frac{\kappa^3}{4m}\sqrt{\frac{1}{2m\Omega(s)}}\left(\hat{a}^\dagger+\hat{a}\right) + V_0 e^{-\gamma s^2} - \frac{\kappa^2}{8m}. \tag{4.20}$$

where the anharmonic parameter χ is included in $\Omega(s)$. Combining Lie Algebra with the Wei-Norman Ansatz brings us to

$$\begin{aligned}
&(\Omega(s))\hat{N} + \left(\frac{\kappa^3}{4m}\sqrt{\frac{1}{2m\Omega(s)}}\right)\hat{a}^\dagger + \left(\frac{\kappa^3}{4m}\sqrt{\frac{1}{2m\Omega(s)}}\right)\hat{a} + \left(V_0 e^{-\gamma s^2} - \frac{\kappa^2}{8m} + \frac{\Omega(s)}{2}\right)1, \\
&= (i\dot{\alpha}_3)\hat{N} + (i\dot{\alpha}_1 - i\dot{\alpha}_3\alpha_1)a^\dagger + (i\dot{\alpha}_2 + i\dot{\alpha}_3\alpha_2)a + (i\dot{\alpha}_4 - i\dot{\alpha}_2\alpha_1 - i\dot{\alpha}_3\alpha_2\alpha_1)1.
\end{aligned} \tag{4.21}$$

where the RHS of (4.21) is the same as in (3.23). Equating the coefficients produces

$$\begin{aligned}
\dot{\alpha}_1 &= i\frac{\kappa^3}{4m}\sqrt{\frac{1}{2m\Omega(s)}} - i\Omega(s)\alpha_1 \\
\dot{\alpha}_2 &= -i\frac{\kappa^3}{4m}\sqrt{\frac{1}{2m\Omega(s)}} + i\Omega(s)\alpha_2 \\
\dot{\alpha}_3 &= -i\Omega(s) \\
\dot{\alpha}_4 &= -iV_0 e^{-\gamma s^2} - i\frac{\kappa^3}{4m}\sqrt{\frac{1}{2m\Omega(s)}}\alpha_1 + i\frac{\kappa^2}{8m} - i\frac{\Omega(s)}{2},
\end{aligned} \tag{4.22}$$

where

$$\Omega(s) = \omega(s) - \chi\left\langle \hat{N}+\frac{1}{2}\right\rangle = \omega(s) - \chi n - \chi\frac{1}{2} + \chi\alpha_1\alpha_2, \tag{4.23}$$

and

$$\omega(s) = \sqrt{\frac{2}{m}\left(D_0\alpha^2 - 3\frac{\kappa^4}{8m}\right)}. \tag{4.24}$$

In this approximation the new effective frequency $\Omega(s)$ becomes a function of the initial vibrational state n. Thus the parametric oscillator adapts also to the chosen initial state through the mean field $\langle\hat{N}\rangle$. The mean-field form of the number operator

$$\left\langle\hat{N}\right\rangle = n - \alpha_1\alpha_2 \tag{4.25}$$

was verified by the computer algebra algorithm seen in Appendix A.4.

The other way we derive a mean-field Hamiltonian is by adding an $\hat{N}^2$ to the Lie algebra. keeping the $\hat{N}^2$ term in the Hamiltonian, and appending this operator to the Lie algebra basis. The new set is no longer a basis for a Lie algebra as the commutation relations do not close in a finite number of steps. The new self-consistent approximation comes from forcing the closure by using expectation values of $\hat{N}$ within the commutation relations, keeping the Morse oscillator anharmonicity in the Hamiltonian. Starting again from (4.19), we can derive the equations of motion the same way. To do this, we note the canonical coefficients for the new 5 dimensional Lie algebra derived in Appendix D.1.3 are needed producing

$$\begin{aligned}
\dot{\alpha}_1 =& -i\frac{\kappa^3}{4m}\sqrt{\frac{1}{2m\omega(s)}} + \alpha_1\left(i\chi - i\omega(s)\right) + i2\alpha_1\chi\langle N\rangle \\
\dot{\alpha}_2 =& -i\frac{\kappa^3}{4m}\sqrt{\frac{1}{2m\omega(s)}} - \alpha_2\left(i\chi - i\omega(s)\right) - i2\alpha_2\chi\langle N\rangle \\
\dot{\alpha}_3 =& i\chi - i\omega(s) \\
\dot{\alpha}_4 =& i\chi \\
\dot{\alpha}_5 =& -iV_0e^{-\gamma s^2} + i\chi\frac{1}{4} - i\omega(s)\frac{1}{2} + i\frac{\kappa^2}{8m} - i\alpha_1\frac{\kappa^3}{4m}\sqrt{\frac{1}{2m\omega(s)}}
\end{aligned} \tag{4.26}$$

as our equations of motion. Note that with the new algebra $\left\langle\hat{N}\right\rangle, \langle\hat{a}\rangle, \left\langle\hat{a}^\dagger\right\rangle$ are all the same as those derived in the previous applications in this dissertation.

In this section we introduced anharmonic behavior into the transverse coordinate. This involved two important steps, one was redefining the oscillation frequency to be dependent on the transverse

coordinate and the other using a mean field.

4.4 Results and Summary

In this section we examine results obtained using the current model. We start with a few standard results to show how the results can be physically relevant and then we move to discuss more peculiar results such as resonance. In the first result shown in Fig. 4.3 we start with a single initial vibrational state for the reactant molecule. After the reaction we see a coherency in the vibration of product molecule.

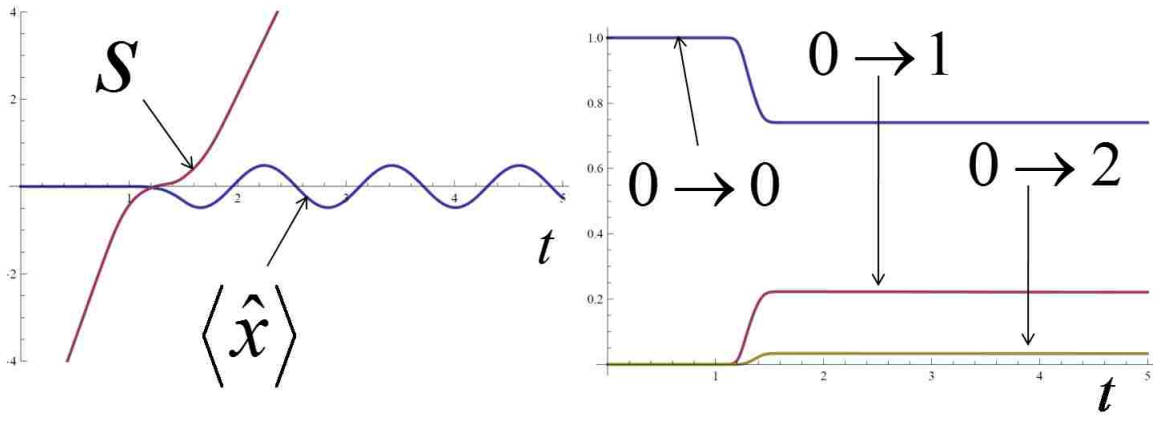

Figure 4.3 The simultaneous collinear trajectory plots and the corresponding transition amplitude using a harmonic oscillator transverse coordinate. The reactant diatomic molecule starts in the ground state. The product molecule gains quanta of energy from the reactive collision.

Fig. 4.6 below is a result that shows how coupling of the translational and transverse coordinates can produce interesting trajectories not seen in previous models.

Most bulk reaction calculation methods assume the transition state can only be crossed once. We show that there are initial conditions, on the molecular scale, where the reaction goes back

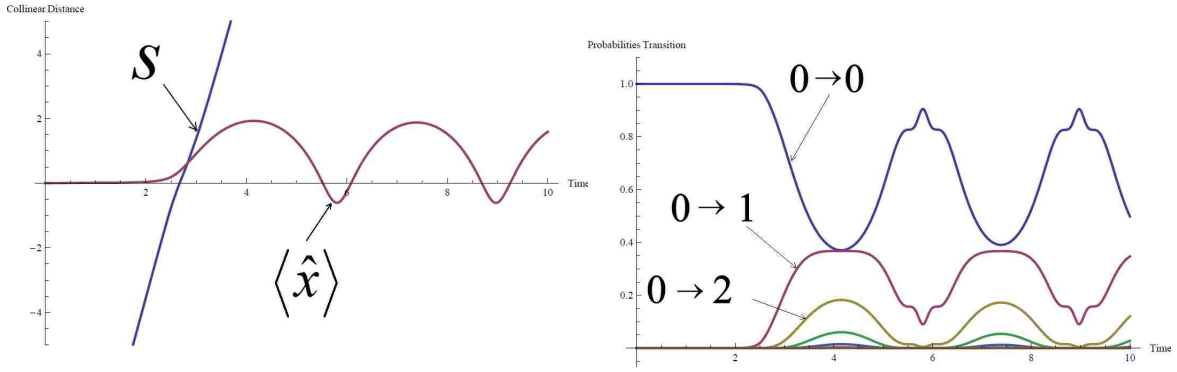

Figure 4.4 Plots of the collinear trajectories of s and $\hat{x}$ from a calculation using mean field theory (4.22) to account for and anharmonic potential.

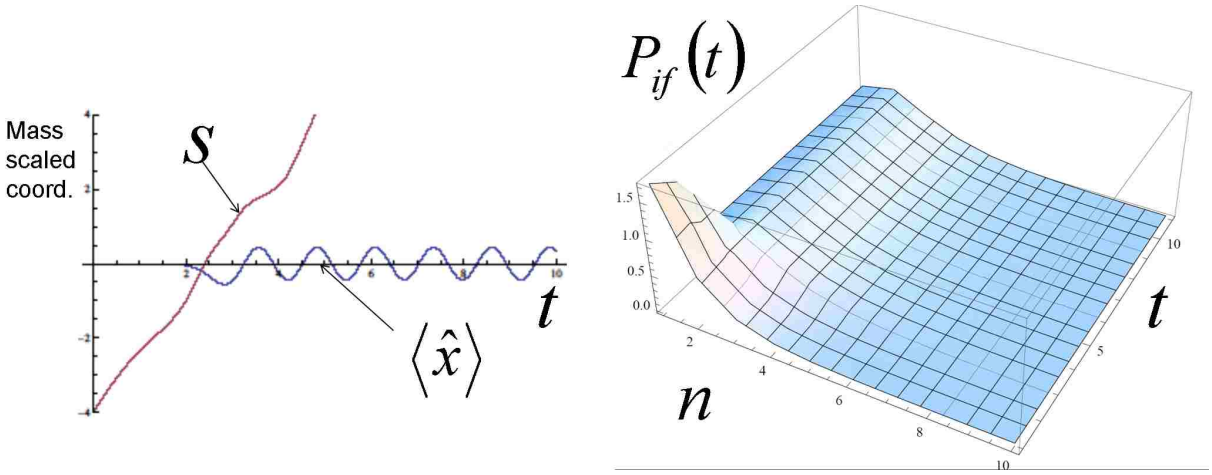

Figure 4.5 The results of applying the harmonic reactive case to an ensemble of collisions. Notice how the collision time in the left plot corresponds to the exact time the Boltzmann distribution is lost on the right plot.

and forth across the potential energy surface saddle point many times. Fig. 4.7 shows resonance around that point from our calculations.

We apply an anharmonic potential in Fig. 4.4 and in Fig. 4.5 the harmonic case is applied to a Boltzmann distribution of molecular energies. The s line in Fig. 4.7 represents where the reaction is relative to the saddle-point which is at zero. Notice how s crosses zero and then comes back The

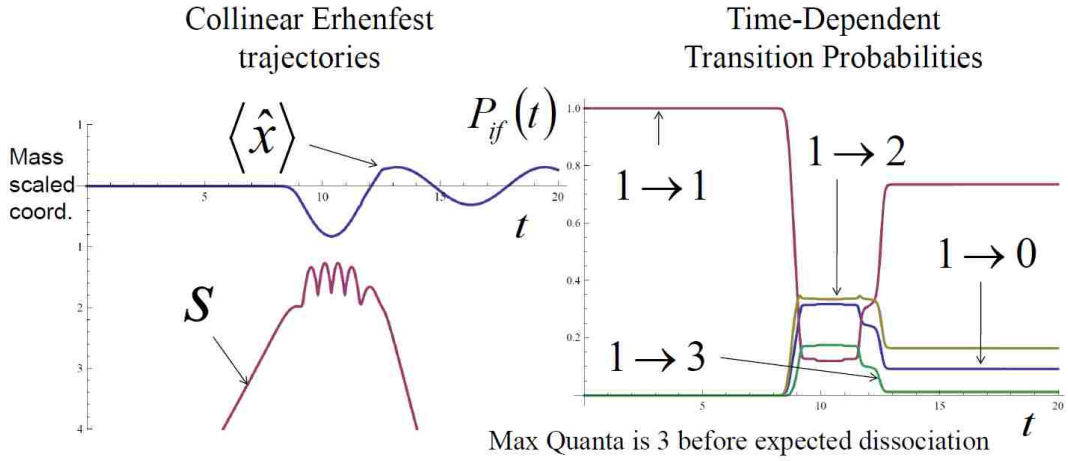

Figure 4.6 Here we see a strong coupling appear as a resonance in the translational coordinate *s*. The plot on the right reveals a brief moment where the state-to-state transition probabilities are slightly inverted. The the parameters chosen in this particular calculation limit the total quanta of vibration number to be 3 before dissociation.

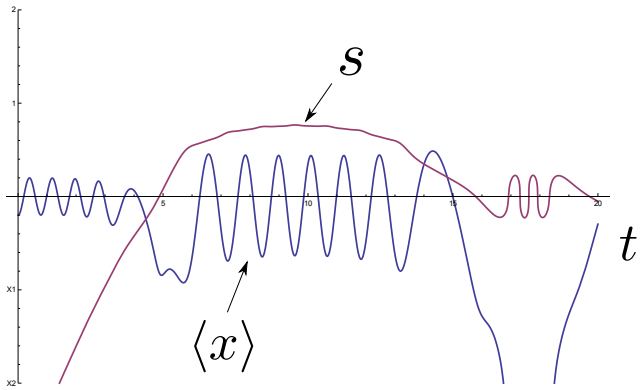

Figure 4.7 Simultaneous plots of the classical and quantum coordinates resonating around the transition state using (4.26).

x line represents how far the reaction has strayed from the minimum energy pathway or reaction coordinate.

In this chapter we saw how the Lie Algebraic method can be applied to inelastic and reactive collisions. The mean field method was needed when we tried to include anharmonic potentials for the $\hat{x}$ coordinate. We also added $\hat{N}^2$ to our algebra which required us to re-derive new standard

coefficients. We also see a simplification in non-equilibrium quantum statistical analysis as the density matrix elements are easily calculated from previous code.

Chapter 5

Summary of Dissertation

When two molecules collide, the interaction is either elastic, inelastic, or reactive. This depends on vibrational energy changes in the molecules and whether there is a rearrangement of the atoms into new species. Beginning with inelastic collisions, we developed a mathematical framework upon which reactive collisions may be accurately modeled.

We used an algebraic method to model molecular collision dynamics. An algebraic structure called the vibron model [18] works as a simple interpretation of a molecule's inner dynamics. Applying Schrodinger's equation and matching coefficients of algebra elements reveals the differential equations-of-motion for each atom in the two colliding species. These equated coefficients are also used to calculate transition probabilities between the internal quantum states of the molecules. It is then possible to compare the trajectories of the atoms with the quantum dynamics of the chemical bonds during the whole collision, which is usually calculated using purely classical approaches.

In our calculations, not all degrees-of-freedom are treated quantum mechanically. For an inelastic collision of an atom and a diatomic molecule, it is not essential to quantize the translational degree of freedom. It is sufficient to treat the relative molecular distance as a classical translational coordinate. However, it's essential we quantize the harmonic motion of the diatomic molecule.

To this end, we explored how the Hamiltonian for a simple triatomic collision is similar to that of an oscillator in a dipole field. We then moved to the more realistic Morse potential to model the diatomic molecule's vibration. Anharmonic behavior emerges and the ability to model complete dissociation of the molecule opens up the door to reactive scattering.

With the Mathematica code optimized for the inelastic and reactive cases, we iterated the model to apply it to an ensemble of atomic collisions with a Boltzmann distribution of molecular vibrational energies. We zoomed in to the non-equilbirium regime and resolved quantum details of the transition state not seen in the literature. Future developments include applications to larger molecular collisions and nuclear reactive scattering.

Appendix A

Computer Code

These 4 programs are referred to through out the dissertation. The first is used in Chapter2, the second is used in Chapter 3, the third is used in Chapter 4, and the fourth is used in all cases.

A.1 Standard Dipole Program

m = 1; wz = 2; l = 3; T = 12 Pi; ImageY = 400; ImageX = 500; W = 1; E0 = 1;

(*Functions={ [[1]] Heaviside at time t = B softness A , \ [[2]] Rectangle in at time t = B out M seconds later, [[3]] Turn on \ an oscillating field at time t = B with softness A,[[4]] Periodic \ Bumps to spikes Spikiness B,[[5]] Sweep up and down frequencies, \ [[6]] Sweep down and up frequencies ,[[7]] sweep from down to up, \ [[8]] sweep from up to down, [[9]] Gaussian pulse wave packet, [[10]] \ Sech squared *)

F[t_, A_, B_, E0_, M_, wz_] := {E0*.5 (Tanh[A (t - B)] + 1) , E0*.5 (Tanh[A (t - B)]) + E0*.5 (-Tanh[A (t - B - M)]), E0 .5 (Tanh[A (t - B)] + 1) Cos[wz t], E0*.5 (Tanh[A t] + 1) Sin[wz t]^(2 B), E0 Sin[A t^(1 + Exp[-(t - B)^2])], E0 Sin[A t^(2 - Exp[-(t - B)^2])], E0 Sin[wz (t - B) (Tanh[(A /20) (t - B)] + 2)], E0 Sin[wz (t - B) (-Tanh[(A /20) (t - B)] + 2)], E0 Sin[wz (t - B)] Exp[-(t - B)^2], E0 Sech[A (t - B)]^2}[[10]];

Amp[m_, n_] := Sqrt[m! n!] Exp[a4[t]] Exp[a3[t] n] Sum[(a2[t]^k/k!) (a1[t]^(m - n + k)/((m - n + k)! (n - k)!)), {k, 0, n}];

Prob[m_, n_] := (Abs[Amp[m, n]]^2)/(Sum[Abs[Amp[j, n]]^2, {j, 0, 8}]); X := Sqrt[1/(2 m W)] (a1[t] - a2[t]); P := -I Sqrt[(m W)/2] (a1[t] + a2[t]);

Manipulate[Module[{alpha = NDSolve[{I a1'[t] == W a1[t] + F[t, A, B, E0, M, wz], I a2'[t] == F[t, A, B, E0, M, wz] - I W a2[t] , a3'[t] == -I W , a4'[t] == -I F[t, A, B, E0, M, wz] a1[t] - I/2 W, a1[-T] == u, a2[-T] == -u, a3[-T] == 0, a4[-T] == 0}, {a1, a2, a3, a4}, {t, -T, T}, MaxSteps -> 90000]}, Grid[{{Show[Plot[{Evaluate[Re[X] /. alpha], F[t, A, B, E0, M, wz]}, {t, -T, T}, PlotRange -> {-1, 1.2}, Frame -> True, PlotStyle -> {{Thick, Black}, {Thick, Black, Opacity[.6]}}, PlotLabel -> Style["Sech Pulse Adiabatic Limit", Large]], ImageSize -> {ImageX, ImageY}], Show[ParametricPlot[{Evaluate[{Re[X], Re[P]} /. alpha]}, {t, -T, T}, PlotRange -> All, PlotStyle -> Thick, PlotLabel -> Style["Sech Pulse Adiabatic Limit Phase space", Large], Frame -> True, FrameLabel -> {"<x>(t)", "<p>(t)"}], ImageSize -> {ImageX, ImageY}], Show[Plot[{Evaluate[Prob[0, 0] /. alpha], Evaluate[Prob[1, 0] /. alpha], Evaluate[Prob[2, 0] /. alpha], Evaluate[Prob[3, 0] /. alpha], Evalu-

ate[Prob[4, 0] /. alpha], Evaluate[Prob[5, 0] /. alpha]}, {t, -T, T}, PlotRange -> {-.1, 1.1}, Frame -> True, FrameLabel -> {"Transition Probability", "Time"}, PlotLabel -> Style["Step Field Adiabatic Limit Transitions", Large], PlotStyle -> {{Thick, Black, Opacity[1]}, {Thick, Black, Opacity[.8]}, {Thick, Black, Opacity[.6]}, {Thick, Black, Opacity[.4]}, {Thick, Black, Opacity[.2]}, {Thick, Black, Opacity[.1]}}], ImageSize -> {ImageX, ImageY}]}]}]], {{A, .16}, .1, 5}, {{B, 0}, 0, 2}, {{u, 0}, -2, 2}, ControlPlacement -> Top]

A.2 Bath of Inelastic Collisions

mA = 1; mB = 3; mC = 1; m = (mA mC)/(mB (mA + mB + mC)); a = 1.3; V = 1.5; ImageY = 300; ImageX = 400; x0 = 40; T = 40; Freq = 2*10^12; NS = 10; Temp = 100; h = 6.626*10^-34; k = 1.381*10^-23; v0 = -4;

Ω:= Sqrt[1 + a^2 V Exp[-a x[t]]]; f1 := a V Exp[a Sqrt[1/(2 Sqrt[1 + a^2 V Exp[-a x[t]]])] Exp[-a x[t]]; yavt := (α_1[t] - α_2[t])/ Sqrt[2 Ω]; pavt := -I (α_1[t] + α_2[t]) Sqrt[Ω/2]; BoltzTrans := v[t]^2 Exp[-(m v[t]^2)/Temp]; vavt := v[t];

ZP[T_, NS_] := Sum[Exp[-(h Freq (n + 1/2))/(k T)], {n, 0, NS}]; Z[T_] := 1/(2 Sinh[(h Freq)/(k T)]);

Amp[m_, n_] := Sqrt[m! n!] Exp[α_4[t]] Exp[α_3[t] n] Sum[(α_2[t]^k/k!) (α_1[t]^(m - n + k)/((m - n + k)! (n - k)!)), {k, 0, n}];

PBF[T_, f_, NS_] := 1/ZP[T, NS] Sum[Abs[Amp[f, n]]^2 Exp[-(h Freq (n + 1/2))/(k T)], {n, 0, NS}];

LieEqns = {x'[t] == v[t], v'[t] == 1/m a V Exp[-a x[t]] Exp[a Sqrt[1/2 Ω] (α_1[t] - α_2[t])], α_1'[t] == -I f1 -I Ω α_1[t], Sα_2'[t] == -I f1 +I Ω α_2[t], α_3'[t] == -Ω, α_4'[t] == -I V Exp[-a x[t]] -I Ω: 2 -I f1 α_1[t]};

Manipulate[Module[{sol = NDSolve[Join[LieEqns, {x[0] == x0, v[0] == Velocity, α_1[0] == 0, α_2[0] == 0, α_3[0] == 0, α_4[0] == 0}], {x, v, α_1, α_2, α_3, α_4}, {t, 0, T}, MaxSteps -> 50000]}, Grid[{{Show[Plot[{Evaluate[Re[yavt] /. sol], Evaluate[Re[x[t]] /. sol]}, {t, 0, T}, PlotRange -> {-3, 8}, PlotStyle -> Thick, AxesLabel -> {Style[Time, Large], Style[Distance, Large]}], ImageSize -> {ImageX, ImageY}], Show[{ListPlot3D[Table[PBF[Tempa, n, NS], {t, 0, T}, {n, 0, NS}] /. sol, PlotRange -> All, PlotStyle -> Yellow, AxesLabel -> {Style[States, Large], Style[Time, Large], Style[Transitions, Medium]}, Mesh -> {Range[0, NS], 0}]}, ImageSize -> {ImageX, ImageY}], Show[Plot3D[PDF[MaxwellDistribution[Abs[v[t]]], v] /. sol, {v, 0, 20}, {t, 0, T}, PlotRange -> All, PlotStyle -> Green, AxesLabel -> {"Speed Distribution", Time, number}, Mesh -> {Range[0, 20], 0}], ImageSize -> {ImageX, ImageY}]}, {Show[Plot[{Evaluate[Abs[v[t]] /. sol], Evaluate[Abs[v[0]] /. sol]}, {t, 0, T}, PlotRange -> {0, 5}, PlotStyle -> {Thick, Dashed}, AxesLabel -> {Time, velocity}], ImageSize -> {ImageX, ImageY}], Show[{ContourPlot[y^2 + 4 Exp[-.3 x + .3 y], {x, -10, 30}, {y, -3, 3}, ContourShading -> None, Contours -> 30], ParametricPlot[{Re[x[t]], Re[yavt] } /. sol, {t, 0, T}, PlotStyle -> {Thick, Black}]}, ImageSize -> {ImageX, ImageY}], Show[Plot[{PDF[MaxwellDistribution[Abs[v0]], v], PDF[MaxwellDistribution[Abs[v[T]]], v] /. sol}, {v, 0, 20}], ImageSize -> {ImageX, ImageY}]}]}]], {{Velocity, v0}, -6, -.5}, {{Tempa, Temp}, 1, 400}, ControlPlacement -> Top]

A.3 Reactive Collision Calculation

ma = 1; mb = 1; mc = 1; M = ma + mb + mc;(* Masses of atoms in kg *)

m = (ma mc)/(mb (ma + mb + mc)); (* Reduced mass of triatomic system in dimensionless \ units *)

Ix = 400; Iy = 300; (* Plot display sizes *)

V0 = 1; γ= 1;(* Parameters of classical reaction coordinate \ potential *)

D0 = 4; β= 2; χ := β^2/(2 m);(* Parameters of \ quantum Morse potential *)

```
Γ= 0;(* Free energy for reaction coordinate *)
b = 6; (* Shape of curvature *)
BL = 0.;(* Location of max curvature along reaction coordinate *)
n = 0;(* Initial quantum state *)
Nmax = Floor[1/β Sqrt[8 m D0] - 1/2];(* Highest bound quantum state *)
T = 20;(* Time window of calculated dynamics *)
V[x_, s_] := V0 Exp[-γ s^2] - Γ Tanh[s] + D0 (1 - Exp[-β x])^2;(* Potential energy of system *)
pVs[x_, s_] := D[V[x, s], s];(* Precalculated partial derivative *)
θ[k0_, b_] := Integrate[ k0/(1 + b^2 (s + BL)^2), {s, -Infinity, Infinity}];(* Mass scaled coordinates assymptotic angle *)
κ[s_] := κ0/(1 + b^2 (s + BL)^2);(* Curvature as a function of classical coordinate *) \
κ0 = k0 /. Solve[θ[k0, b] == ArcTan[Sqrt[M mb/(ma mc)]], k0][[ 1]];(* Curvature coefficient calculated from masses *)
Re[θ[κ0, b] 360/(2 Pi)];(* Mass scaled coordinates assymptotic angle \ specified *)
pks[s_] := D[κ[s], s];(* Precalculated partial derivative *)
Amp[m_] := Sqrt[ m! n!] Exp[α5[ t]] Exp[α4[t] n^2] Exp[α3[ t] n] Sum[(α2[t]^k/ k!) ( α1[t]^(m - n + k)/((m - n + k)! (n - k)!)), {k, 0,
n}];(* Transition amplitude of diatomic molecule *)
Pif[m_] := Abs[Amp[m]]^2 ;(* Transition probability *)
ω[s_] := Sqrt[2 D0 β^2/ m - (3 κ[s]^4)/(4 m^2)];(* System zero point frequency as a function \ of classical coordinate *)
xavt := (α1[t] - α2[t]) Sqrt[ 1/(2 ω[s[t]] m)];(* Expectation value of quantum postion operator *)
pavt := -I (α1[t] + α2[t]) Sqrt[ m ω[s[t]] / 2];(* Expectation value of quantum momentum operator *)
h := κ[s[t]]^3/(4 m) Sqrt[ 1 /(2 m ω[s[t]])];(* Function used multiple times *)
Nave := n - α1[t] α2[t];
LieEqns = {
s'[t] == ps[t]/(m ((1 +κ[s[t]] xavt))^2), ps'[t] == (xavt ps[t]^2/((m (1 + κ[s[t]] xavt)^3 ))) pks[ s[t]] - pVs[xavt, s[t]],
α1'[ t] == -I h + α1[t] (I χ- I ω[s[t]] ) + 2 I α1[t] χNave,
α2'[ t] == -I h -α2[t] (I χ- I ω[s[t]] ) - 2 I α2[t] χ Nave,
α3'[t] == I χ- I ω[s[t]] ,
α4'[t] == I χ,
α5'[ t] == -I V0 Exp[-γ s[t]^2] + .25 I χ- .5 I ω[ s[t]] + I κ[s[t]]^2/(8 m) - I α1[ t] h};(* System of coupled partial differential equations *)
Manipulate[Module[{Solution = NDSolve[Join[LieEqns, { s[0] == -6, ps[0] == v, α1[0] == Combo, α2[0] == -Combo, α3[0] == 0, α4[0]
== 0, α5[0] == 0}], {s, ps, α1, α2, α3, α4, α5}, {t, 0, T}, MaxSteps -> 10000, Method -> {StiffnessSwitching, Method -> {ExplicitRungeKutta,
Automatic}}, AccuracyGoal -> 3, PrecisionGoal -> 3]}, Grid[{{Show[ Plot[Evaluate[{Re[xavt], Re[s[t]]} /.  Solution], {t, 0, T}, PlotRange -
> {-4, 4}, PlotStyle -> Thick], ImageSize -> {Ix, Iy}], Show[Plot[{Pif[0] /.  Solution, Pif[1] /.  Solution}, {t, 0, T}, PlotRange -> {-.1, 1.1},
PlotStyle -> {Thick}], ImageSize -> {Ix, Iy}], Show[{ContourPlot[V[x, s], {x, -.4, 1}, {s, -8, 8}, PlotRange -> {{-.4, 1}, {-8, 8}}, Contours ->
20], ParametricPlot[{-\[Kappa][s] + 1, s}, {s, -6, 6}, PlotStyle -> {Blue, Thick}], ParametricPlot[ Evaluate[{Re[xavt], Re[s[t]]} /. Solution], {t, 0,
10}, PlotStyle -> {Red, Thick}]}, ImageSize -> {Ix, Iy}]}}]], {{v, .88, "Starting Speed"}, .1, 6, Appearance -> "Labeled"}, {{Combo, 0, "Starting
Combo"}, 0, 1, Appearance -> "Labeled"}, ControlPlacement -> Top]
```

A.4 Computer Algebraic Manipulations

by Ty Beus and Manuel Berrondo

```
(*The program should work for any given Lie Algebra.*)
basis = {aa, a, num, num2, id};
nobasis[x_] := And @@ (FreeQ[x, #] & /@ basis);
(* properties of commutators *) (* id is the identity opertor *)
Clear[X];
X[a, aa] = id;
X[a, num] = a;
X[aa, num] = -aa;
X[a, num2] = 2*nav*a; (* a**num+num**a;*)
X[aa, num2] = -2*nav*aa; (* -aa**num-num**aa; *)
X[x_, id] := 0;
X[id, x_] := 0;
X[x_, x_] = 0;
X[c_?nobasis, x_] := 0;
X[x_, y1_ + y2_] := X[x, y1] + X[x, y2];
X[c_?nobasis * x_, y_] := c*X[x, y];
X[x_, c_?nobasis] := 0;
X[y1_ + y2_, x_] := X[y1, x] + X[y2, x];
X[y_, c_?nobasis * x_] := c * X[y, x];
X[x_, y_] := -X[y, x] /; OrderedQ[{y, x}];
collC[x_] := Collect[x, basis];
(* properties of noncommutative product *)
prot = Unprotect[NonCommutativeMultiply];
(* mixed properties *)
X[x_ ** y_, z_] := x ** X[y, z] + X[x, z] ** y;
X[x_, y_ ** z_] := y ** X[x, z] + X[x, y] ** z;
X[x_ * y_, z_] := x ** X[y, z] + X[x, z] ** y;
X[x_, y_ * z_] := y ** X[x, z] + X[x, y] ** z;
id ** x_ := x;
x_ ** id := x;
(-y_ ) ** z_ := -y ** z;
y_ ** (-z_) := -y ** z;
c_?nobasis ** z_ := c* z;
z_ ** c_?nobasis := c* z;
(c_?nobasis * p_) ** z_ := c* (p ** z);
```

```
z_ ** (c_?nobasis * p_) := c* (z ** p);
(y1_ + y2_) ** z_ := y1 ** z + y2 ** z;
z_ ** (y1_ + y2_) := z ** y1 + z ** y2;
y_ ** -z_ := -y ** z;
Protect[ Release[prot]];
dim = Length[basis];
αα= Table[α[i][t], {i, dim}];
dαα= D[αα, t];
(* "Hamiltonian:"*)
hamOsc = (num + (1/2)*id) ω;
ham0 = hamOsc + χ (num2 + num + (1/4)*id ) ω;
ham = ham0 + g[t] (a + aa)
(*e^{p×}Q*)
(* note M = px operator when the thing it is being applied to is in vector form under the Lie algebra basis *)
expCross[P_, Q_] := Module[{v, MTr},
   MTr = Table[ Coefficient[X[P, basis[[i]]], basis[[j]]], {j, dim}, {i, dim}];
   v = Table[Coefficient[Q, basis[[j]]], {j, dim}];
   MatrixExp[MTr, v].basis]
(* DUInvU writes U'*U^-1 in terms of the Lie algebra *)
DUInvU[Alg_] := Module[{v, dimA}, dimA = Length[Alg]; Sum[v = Reverse[dαα][[i]]*Reverse[Alg][[i]];
   For[j = dimA - i + 1, j >= 1, j–, v = expCross[αα[[j]]*Alg[[j]], v]]; v , {i, dimA}]]
(* "Find U' in terms of the Lie algebra" *)
DUInvUsol = collC[DUInvU[basis]]
(* "Find the Differential Equations for α's" *)
(* U'*U^-1 + I*H = 0 we match Lie coefficients to set up differential equations to find α's*)
eq1 = Flatten[ Table[{Coefficient[DUInvUsol + I*ham, basis[[i]]] == 0}, {i, dim}]];
rhs = Flatten[dαα/. Solve[eq1, dαα]];
eom = Table[dαα[[i]] == rhs[[i]], {i, dim}]
initCond = Table[αα[[i]] == 0 /. t -> 0, {i, dim}];
eqsD = Join[eom, initCond];
(* sol=FullSimplify[DSolve[eqsD,αα,t]] *)
```

Appendix B

Background of Molecular Collision Theory

I have found the following topics to be essential in understanding why the model developed in this dissertation is important.

B.1 Collisions in the Bulk

In a gas there are relatively large amounts of space between the colliding gas particles. At STP[1], the mean-free-path of diatomic nitrogen is three orders of magnitude greater than its Van der Waals radius. There exists distinct time scales with which molecules are in and out of contact with each other. We want to model what happens while they are in contact. We develop a detailed model for single collisions because the large mean-free-path validates the iteration of single collisions when modeling macroscopic gas properties. There is behavior in the macroscopic world that is explained only by the theory of individual molecular collisions.

Equations of state, like the ideal gas law, are sufficient in explaining macroscopic variable relations, like temperature and pressure. However, the ideal gas law does not include interactions

[1] IUPAC established standard temperature and pressure (informally abbreviated as STP) as a temperature of 273.15 K (0 °C, 32 °F) and an absolute pressure of 100 kPa (14.504 psi, 0.987 atm, 1 bar)

between the gas particles, which can be a limiting factor. The Van der Waals equation is a step toward a more correct equation of state, as it takes into account the nonzero size of molecules and the interactions between them.

It is necessary to include energy transfer and relaxation of internal degrees-of-freedom for accurate predictions of interacting systems. In some cases, such as population inversion for lasing, combining statistical mechanics principles with details of the individual molecular collisions is the only way to explain certain macroscopic behavior. Acknowledgment of complex molecular interactions in a gas is essential in the agreement of theory and experiment in some cases.

There are three ways molecules collide: elastically, inelastically, and reactively. In the elastic collisions the relative translational kinetic energy before and after the collision is the same. In the case where the translational kinetic energy changes, this would be considered an inelastic collision, as the initial and final states of the species internal degrees-of-freedom are different. Inelastic collisions are most noticeable when the relative translational kinetic energy changes significantly. During an inelastic molecular collision, any or all of the electronic, rotational, vibrational, and translational energies of the colliding species can change. In a reactive collision, even more possible outcomes arise. Not only is it possible for all these internal degrees-of-freedom to change state, but now they're redistributed in a new molecule. The reactive collision is what we aim to model in this dissertation.

B.2 The Molecular Forces Involved

Imagine a vibrating diatomic molecule mathematically reduced to a single oscillating mass μ. Treating this system as simple harmonic oscillator has its limitations. There are features of this diatomic molecule that Hooke's law fails to model such as the observed uneven spectrum of energy levels. The Morse potential [21]($\hbar = 1$),

$$V_{\mathrm{M}} = D_0 \left(1 - e^{-\alpha x}\right)^2, \tag{B.1}$$

produces the Morse spectrum

$$E_{\mathrm{M}} = \omega \left(n + \frac{1}{2}\right) - \omega\chi \left(n + \frac{1}{2}\right)^2, \tag{B.2}$$

where

$$\omega = 2\alpha\sqrt{\frac{D_0}{2\mu}} \qquad \text{and} \qquad \omega\chi = \frac{\alpha^2}{2\mu} \tag{B.3}$$

for an oscillating reduced mass μ. The Morse Potential is more accurate for the interaction of atoms in diatomic molecules than the harmonic oscillator [8,9,13] . It allows for three important dynamic results: simple harmonic motion at low energies, anharmonic at high energies, and dissociation at super high energies.

For example, Fig. B.1 shows the potential energy for the HCl molecule, fit to experimental data. The Morse potential produces vibrational spectra for diatomic molecules so well that it is the choice analytic form for the convergence of theoretical and experimental standards in the field of molecular spectroscopy. NIST provides molecular data in terms of the simple fitting parameters D_0 and α for the spectrum of a Morse potential[2].

In our calculations there are also weaker intermolecular forces to consider called Van der Waals

[2]http://webbook.nist.gov/cgi/cbook.cgi?ID=C7647010&Mask=1000

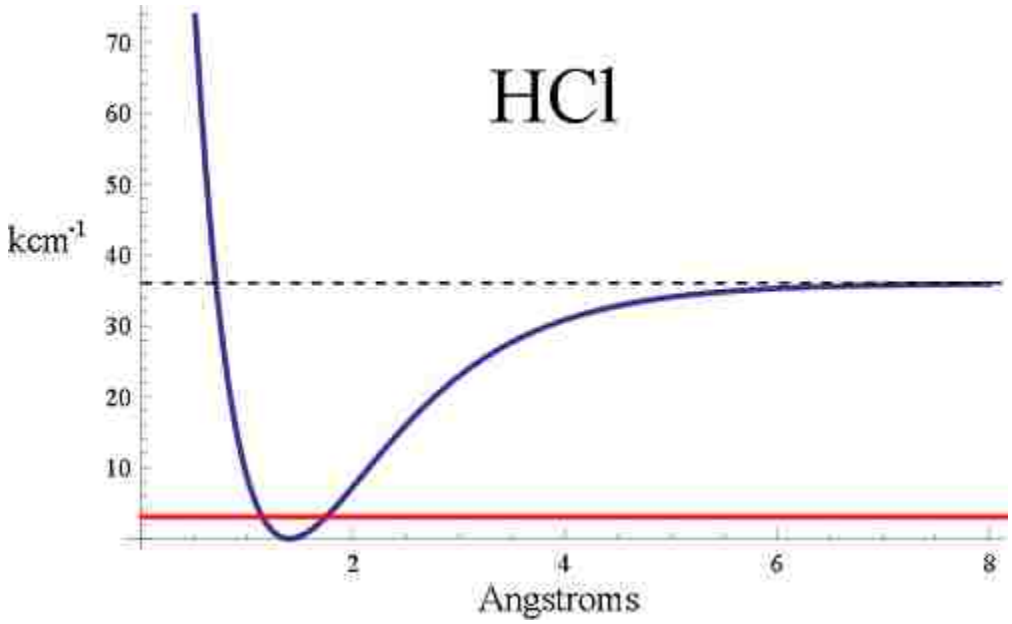

Figure B.1 The Morse potential energy function for an HCl molecule. The dotted line represents the dissociation energy of 36,000 cm^{-1}. The zero-point energy of 3000 cm^{-1} is shown with the red line. This figure was generated with data from NIST.

forces[3]. Generally the intermolecular forces are repulsive for collinear inelastic collisions and can be modeled with exponential functions, such as in the Landau-Teller model. However, in reactive collisions a potential energy surface with a saddle-point (activation energy), models the collision where the asymptotic reactant and product channels are on either side.

B.3 The Potential Energy Surface

For all molecular interactions there exists a potential energy "surface" for the electronically adiabatic motion of the nuclei. In a collinear triatomic collision the potential energy surface is easily visible because there are only two degrees-of-freedom. To begin deriving a potential energy surface for our collinear triatomic system, we first define the coordinates to be separations between

[3]The Nobel Prize in Physics 1910 was awarded to Johannes Diderik van der Waals "for his work on the equation of state for gases and liquids".

particles: R_{AB} and R_{BC}, in Fig. B.2.

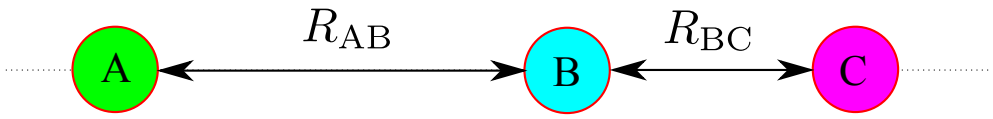

Figure B.2 Collinear coordinates for a triatomic system.

These collinear coordinates will be used for both the inelastic and reactive cases in this dissertation. It is a one-dimensional space with two degrees-of-freedom R_{AB} and R_{BC}, excluding the centers-of-mass.

B.3.1 The Motivation Behind the Collinear Triatomic System

The energy spacing for rotational spectra of diatomic molecules is continuous compared to the vibrational energy spacings. In general, the energy levels involved in V-T (vibration-to-translation) transfer are far greater than those in any energy transfer involving rotations. The R-T (rotation-to-translation), T-R (translation-to-rotation), R-V (rotation-to-vibration), and V-R (vibration-to-rotation) energy transfers are all assumed to be adiabatic because of these large differences in time and energy scales.

THE STERIC FACTOR

In many systems there are favored orientations for the reaction to occur. For example, each of the four sides of the methane has a cone-of-acceptance that represents the solid angles in which Methane is most vulnerable to reacting.

A reaction where one of the Hydrogen atoms in the methane is replaced by an incoming free hydrogen, is most likely to occur when the incoming Hydrogen approaches the methane along the axis of one of these cones. One axis in particular is in yellow in Fig. B.3. If we were to

calculate reactive collision rates for methane we would calculate the dynamics along this yellow axis. We calculate the dynamics along this collinear coordinate because this is the orientation where a reaction is most likely to occur.

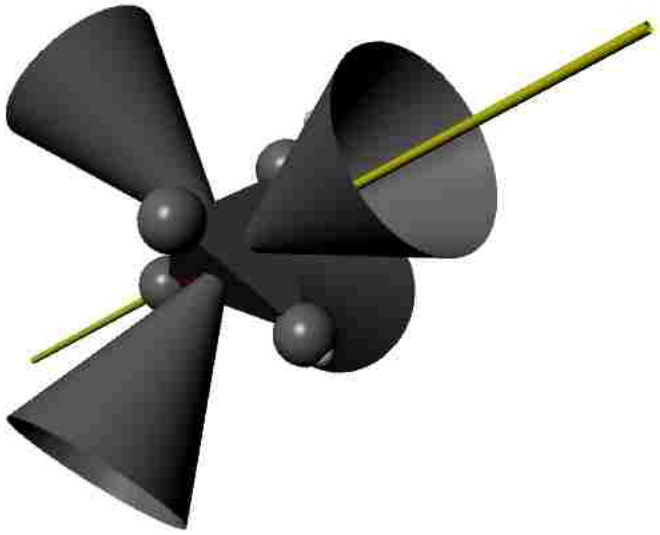

Figure B.3 Cones of acceptance for a methane moleucule shown in grey. Shown in yellow is the prefered axis along which one may construct a collinear collision calculation.

We choose to calculate reactive collisions in a linear triatomic system oriented in a particular way because it enhances the probability of a reaction. Using the other orientations would most likely result in an inelastic collision rather than reactive scattering.

B.4 Inelastic Collisions

A simple example of a triatomic inelastic collision would have a potential energy surface with an oscillator valley in R_{BC}, and a repulsive exponential wall in R_{AB} at only one end of the valley. This surface is shown as a contour plot in Fig. B.4. The classical motion of the three atoms can be

reduced to that of a single mass m sliding across this frictionless surface [12, 24]. The motion of the colliding particles is then interpreted by imagining this single-mass as a bobsled on a track.

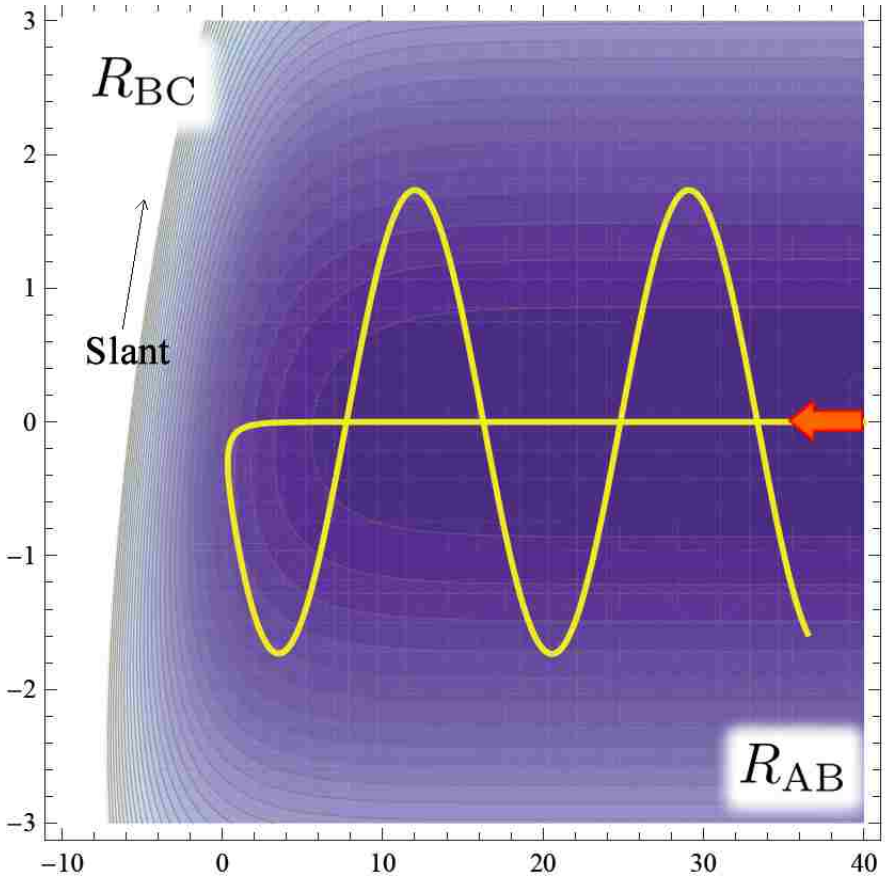

Figure B.4 The contour plot of the potential energy surface for a collinear triatomic inelastic collision.

A good example of this bobsled trajectory is seen in the yellow line in Fig. B.4. In this case, the sled has the initial condition (orange arrow) of being at the bottom of the valley and far away from the wall. Physically, this transforms back to atom A being very far away from, but approaching, the non-oscillating diatomic molecule BC. When the sled goes up the exponential wall, the slant in the potential energy surface pushes it to the side. It is due to this push, that as the sled goes back

down it is also sliding back and forth across the valley. This corresponds to vibrationally exciting the BC molecule. The velocity in the R_{AB} direction decreases as this inelastic collision has resulted in T-V (translational to vibrational) energy transfer. It is important to note that the transformation into the "single mass" coordinates produces a slight slant in the repulsive wall seen on the left side of Fig. B.4. Without this slant, vibrational excitation would be more difficult.

To summarize, in nonreactive collisions, particles collide somewhere between elastically and inelastically, never resulting in dissociation of bonded atoms. At one end of the spectrum, the elastic collisions involve no exchange of energy between the two colliding particles. At the other end, inelastic collisions do exchange energy. Therefore some degrees-of-freedom lose or gain energy during an inelastic collision. The energy terms E in Fig. B.5 each have a subscript denoting the type of energy they represent. The subscripts are e,t,r, and v, which stand for electronic, translational, rotational, and vibrational respectively. Fig. B.5 is a depiction of the process we are focusing in on.

After the inelastic collision, the density of each of these states changes. For example, in Fig. B.5 the methane molecule could lose some translational energy giving it to one of the normal vibrating ammonia modes. The collinear triatomic system can be seen by freezing out the appropriate degrees of freedom in the intermediate stage of Fig. B.5 during the small time-scale in which the reaction takes place. In this dissertation we develop a mathematical model that follows the details of how the vibrational state changes throughout the collision by focusing on the collinear triatomic system.

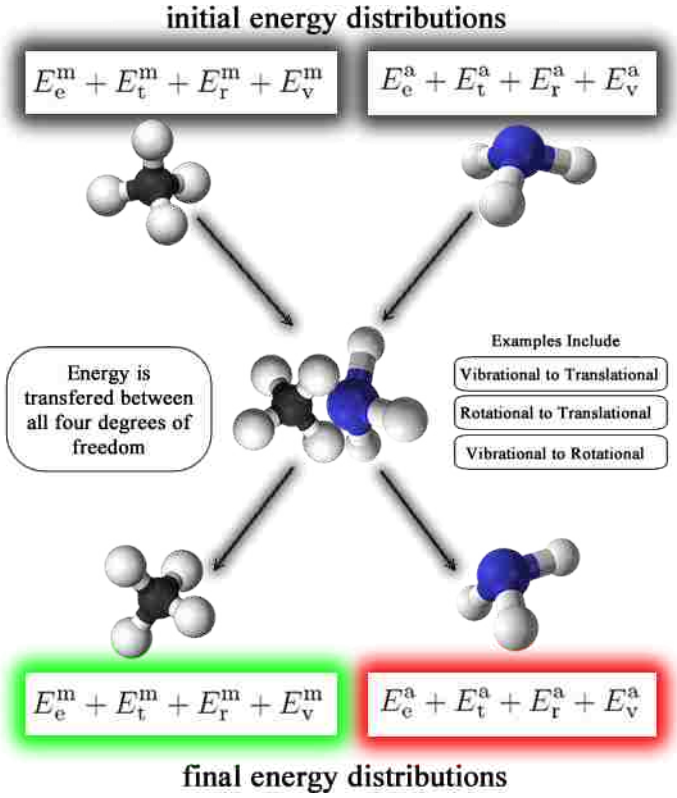

Figure B.5 A schematic for energy transfer during an inelastic molecular collision.

B.5 Reactive Collisions

Consider a non-reacting mixture of two different molecules. If there exists a different molecular configuration that is lower in energy, then there exists an activation energy which is necessary to add to the system in order for the individual molecules to recombine into this new stable configuration. This new configuration is obtained by following a "reaction coordinate," which smoothly connects reactants to products. Upon recombining, new bonds form and the system will release the "exergic" energy, which is the activation energy plus the free energy seen as a drop after passing the transition state of the reaction coordinate in Fig. B.6.

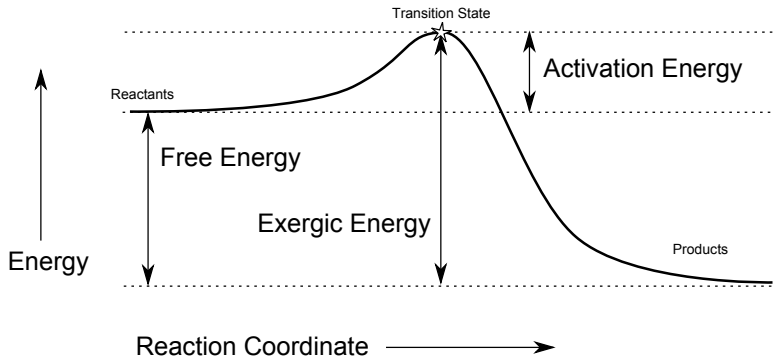

Figure B.6 The reaction coordinate dependance on energy.

The depiction of the energy levels in a reaction in Fig. B.6 is oversimplified. A real reaction coordinate is a curve in higher dimensional space extracted from the potential energy surface. The reaction coordinate is a minimum energy pathway (the red line in Fig. B.7) between reactant and product channels that has a local maximum (activation energy). The simplest surface on which to visualize a reactive collision is a collinear triatomic system. Fig. B.7 is a contour plot of the potential energy surface for 3 hydrogen atoms interacting. With three atoms in a collinear configuration, we can model the collision dynamics with a single mass on a frictionless surface just like the inelastic example above, except this surface has a saddle point over which a reaction can occur.

Note the reflection symmetry across $R_{\mathrm{AB}} = R_{\mathrm{BC}}$ as expected for three hydrogen atoms. You can also see the Morse potential shape in the valleys where the individual diatomic molecules are isolated (top left and bottom right). Also note that there is not a specific trajectory shown on this surface like on the inelastic surface contour plot in Fig. B.4. This contour place is a cartoon representation for the real surface which would essentially be skewed into a mass-scaled coordinate system. The red line is the minimum energy path from the reactant channel, across the saddle point, and into the product channel. This path will be used as a curvilinear "reaction" coordinate later on.

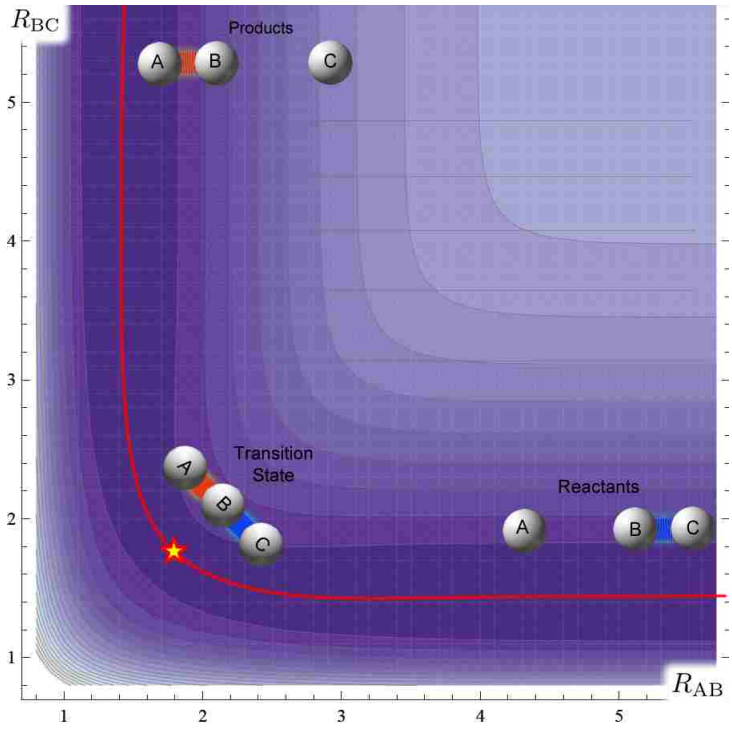

Figure B.7 A contour plot of the potential energy surface for the interaction of 3 hydrogen atoms.

Modern molecular spectroscopy techniques (femtochemistry) allow conditions for a reaction to be observed in detail. When isolated, the reactant and product species have unique vibrational spectra. When mixed, the reaction A+BC→AB+C takes place and their spectral features combine, and new lines may appear. These spectral changes continue to appear even after the forward reaction is over. The "?" in Fig. B.8 is the spectrum of the transition state for the reaction. This is the spectrum that femtochemistry experiments try to resolve.

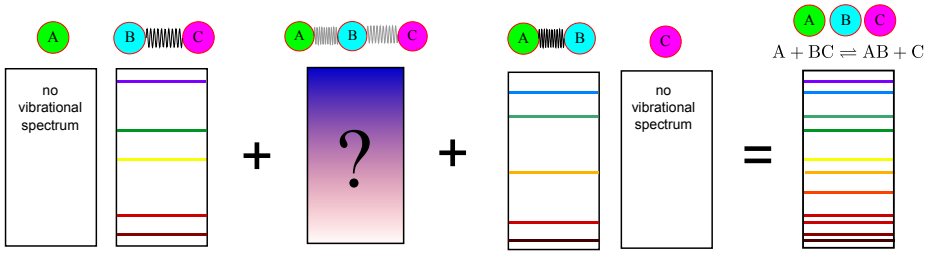

Figure B.8 The emission spectra at each three important comfigurations through out a reaction.

In dynamic equilibrium, the rate at which product species are being formed equals the rate at which the reactant species are being formed, A+BC⇌AB+C. This means there is a steady occurrence of the transition state. Ambitious experimental scientists such as Zewail who was awarded the 1999 Nobel Prize in Chemistry have shown that we can observe this transition state with fluorescence [25].

To summarize, imagine a chemical reaction between carbon monoxide and nitrous oxide:

$$CO + N_2O \rightarrow CO_2 + N_2. \tag{B.4}$$

Fig. B.9 is a cartoon depiction of the dynamics of (B.4). After the reaction, the occupancy of each of these states changes. In this dissertation we attempt to model the reactive collision to include the details on how the vibrational state changes by focusing on the collinear triatomic system.

B.6 Non-equilibrium Statistical Mechanics

To truly take advantage of our calculation we apply it to an ensemble of collisions. Consider a bath of diatomic molecules and atoms in thermal equilibrium as they repeatedly collide with each other. In a thermally equilibrated microcanonical ensemble all 4 degrees-of-freedom, electronic, translational, rotational, and vibrational each share 1/4 of the total energy.

$$E_{\text{tot}} = E_{\text{e}} + E_{\text{t}} + E_{\text{r}} + E_{\text{v}} \tag{B.5}$$

In our work, we only consider two terms, translational and vibrational. The atom-atom collisions are taken to be elastic, therefore, over the duration of the atom-diatom collision, there is no

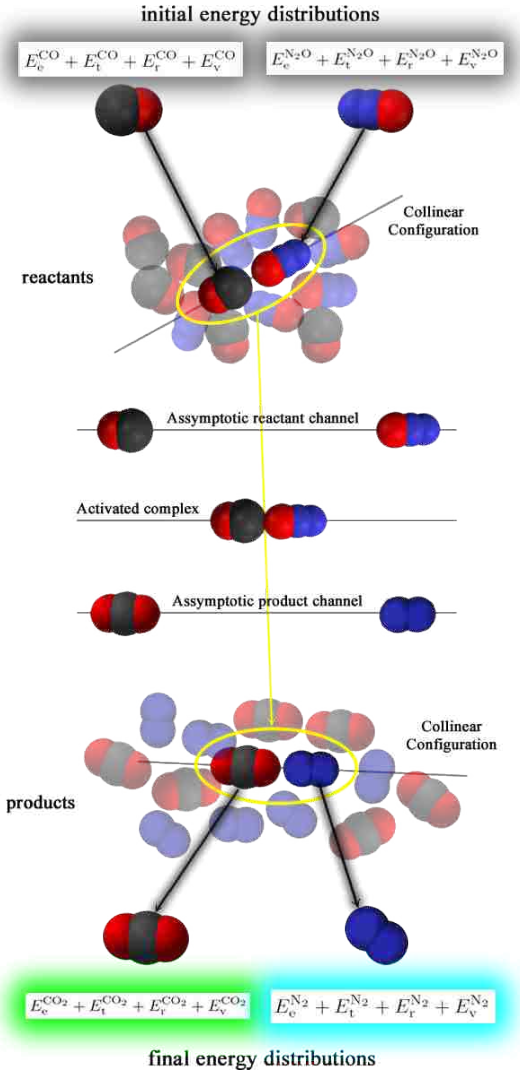

Figure B.9 A schematic of energy transfer during a reactive molecular collision.

change in the Maxwell-Boltzmann speed distribution of the atoms. In our calculations, we consider a canonical ensemble of oscillators initially in thermal equilibrium, exchanging energy with a heat bath (collisions with the atoms). During this energy exchange via inelastic collisions, they temporarily leave thermal equilibrium with the bath.

The equipartition theorem tells us that initially under thermal equilibrium the average energy for each oscillator is $\frac{1}{2}kT$ and for each relative translational kinetic energy is $\frac{1}{2}kT$. Therefore, just after an inelastic collision, the average for the whole ensemble of both degrees-of-freedom

unequally divides the total kT energy. However, upon relaxation back to thermal equilibrium, the equipartition becomes valid again. It must then be stated that the mean kinetic energy of gas molecules is not the same thing as a distribution of energies. It is the distribution that leaves thermal equilibrium.

A distinction between microcanonical and canonical ensembles is essential here. If we consider the whole system, a microcanonical ensemble, we stay on a constant energy surface in phase-space. In microcanonical ensembles, an average overall system temperature may be undefined. We assume no initial thermal equilibrium, as it is necessary that the two degrees-of-freedom be unequal in energy for any net microscopic dynamics to take place. During this process of relaxation, while thermal equilibrium occurs, an overall system temperature becomes defined.

We treat the system as a canonical ensemble of oscillators disturbed by collisions, so the opposite occurs. In this case, we begin with a defined temperature in the form of a Boltzmann distribution of initial conditions for the bath of harmonic oscillators. Then the system leaves thermal equilibrium after this statistical ensemble of single inelastic collisions takes place. It is important to note that the whole system is in thermal equilibrium the whole time as the rate at which inelastic collisions are forcing V-T transfers stays equal to the rate at which inelastic collisions are forcing T-V transfers. Since V-T relaxation is usually significantly slower than V-V relaxation, we essentially have a negligible deviation from thermal equilibrium between the two interacting harmonic oscillator baths over the duration of the atom-diatom collision. This is one of many adiabatic approximations needed in this calculation. Among the others are Born-Oppenheimer (electronic adiabaticity), T-T relaxation (assumed to be much slower) and R-R relaxation (assumed to be much faster). A formal derivation of a canonical ensemble is done by taking the partial trace of a microcanonical ensemble, integrating out the heat bath degrees-of-freedom.

After an inelastic collision, the original Maxwell-Distribution for the relative speeds $f(v,T) \propto v^2 e^{-\frac{mv^2}{kT}}$ will redistribute in general, depending on if the collision is a T-V transfer(a) or a V-T

transfer(b) seen in Figure B.10.

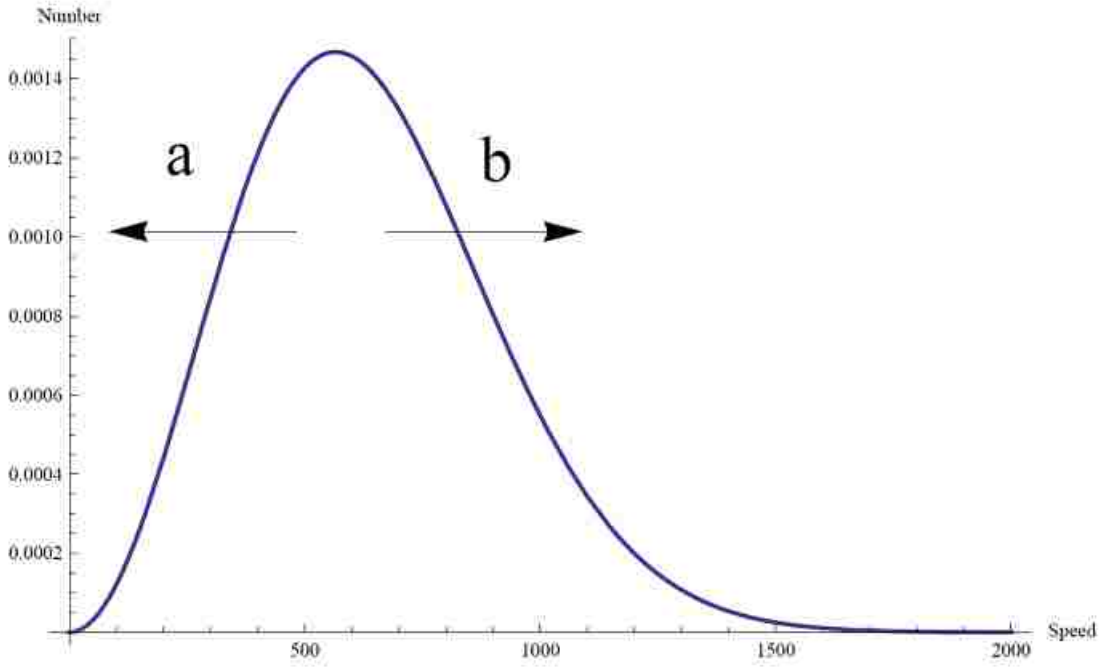

Figure B.10 Redistribution of particles initially in thermal equilibrium.

On the other hand, the Maxwell-Boltzmann distribution for the diatomic molecule vibrational states $g(n,T) \propto e^{-\frac{\hbar\omega\left(n+\frac{1}{2}\right)}{kT}}$, in general, is redistributed the opposite way in Figure B.11. This is the distribution we use in our calculations.

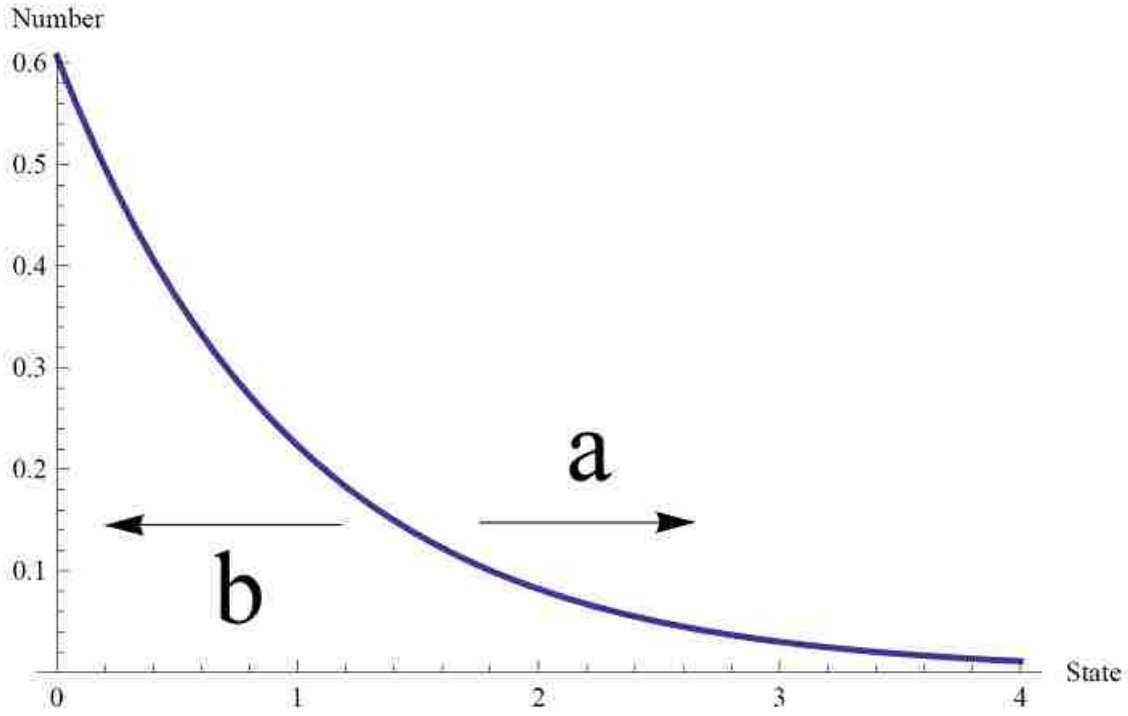

Figure B.11 Corresponding shift in distribution of oscillator states.

B.6.1 Canonical Ensemble of initial conditions

The goal of this dissertation is to be able to apply calculations of many single collisions to a canonical ensemble, and this involves partition functions. The quantum harmonic oscillator partition function in the limit of infinite oscillators is

$$Z(T) = \frac{1}{\sinh\left(\frac{\hbar\omega}{kT}\right)}. \tag{B.6}$$

The Boltzmann distribution for this canonical ensemble of Q.H.O. is

$$\Xi = \frac{1}{Z} e^{-\hbar\omega\left(n+\frac{1}{2}\right)/kT}. \tag{B.7}$$

The transition amplitude for the oscillator to move from n to m is found with computer algebra systems to be

$$A = \sqrt{m!n!}e^{\alpha_4}e^{n\alpha_3}\sum \frac{\alpha_2^k}{k!}\frac{\alpha_1^{m-n+k}}{(m-n+k)!\,(n-k)!}. \tag{B.8}$$

We may then iterate over all possible combinations to get

$$P_{if} = |A|^2 e^{-\hbar\omega\left(n+\frac{1}{2}\right)/kT}. \tag{B.9}$$

Appendix C

Essentials of Quantum Dynamics

I have found that the following appendix entries are very important for understanding the results of this dissertation.

C.1 Stationary States

A quantum state can be made of single “kets” $|\psi_1\rangle$, "bras” $\langle\psi_1|$ or “wave functions” $\psi_1(x)$. These are defined as “single states”. A quantum state may also be composed of a “superposition” of kets

$$|\Psi\rangle(t) = \sum_{n=0}^{\infty} c_n |\psi_n\rangle e^{-\frac{i}{\hbar}E_n t} \tag{C.1}$$

bras

$$\langle\Psi|(t) = \sum_{n=0}^{\infty} c_n \langle\psi_n| e^{-\frac{i}{\hbar}E_n t} \tag{C.2}$$

or wave functions, which are just bras or kets projected into position or momentum space

$$\langle x|\Psi\rangle(t) = \Psi(x,t) = \sum_{n=0}^{\infty} c_n \psi_n(x) e^{-\frac{i}{\hbar}E_n t} \tag{C.3}$$

When squaring the wave function new properties emerge.

$$|\langle\Psi|\Psi\rangle|^2 = \textstyle\sum_{n,m} c_n \langle\psi_n|\psi_m\rangle c_m^* e^{-\frac{i}{\hbar}(E_n - E_m)t} \tag{C.4}$$

$$= \textstyle\sum_n c_n c_n^* \langle\psi_n|\psi_n\rangle + \sum_{m\neq n} c_n c_m^* \langle\psi_n|\psi_m\rangle e^{-\frac{i}{\hbar}(E_n - E_m)t}$$

The second term in eqn. (C.4) carries the time-dependence. If only one coefficient is nonzero the probability will be independent of time and the associated state is called "stationary". When more than one coefficient is nonzero that a superposition is squared and the second term carries the "interference" between the superposed states. The state then has "coherent" behavior as the phase information is carried in the double sum.

C.2 Graphical Explanation of Stationary States

The solutions to Schrodinger's Time-Independent Equation,

$$\hat{\mathscr{H}}\Psi = E\Psi \tag{C.5}$$

are stationary states. In figure C.1 we have plotted probability densities for the harmonic oscillator at 8 different energies. Stationary states are defined by a single energy. For example, the quantum harmonic oscillator single state energy is depicted as the darker horizontal red line at $n = 2$. Since this is the time-independent solution, the darker vertical red line representing the expectation value never moves. The lighter red lines in figure C.1 are upper and lower bounds of uncertainty and they never move either. Also, note that as you increase energy levels for single states the position expectation value stays centered right at zero, while the uncertainties broaden.

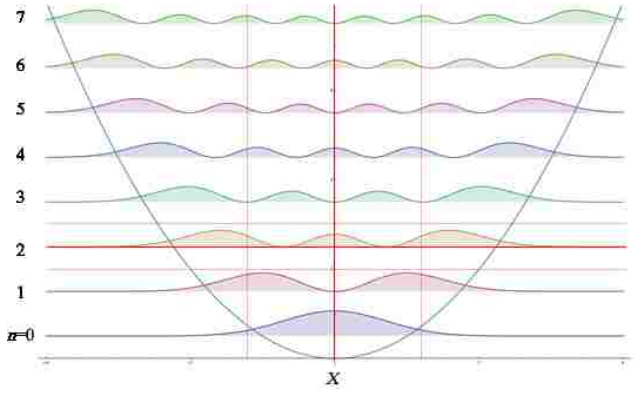

Figure C.1 Expectation values for energy and position in a harmonic oscillator.

Figure C.2 shows an anharmonic oscillator potential and the first 5 energy eigenstates for the potential. Consider a single state of energy 2. As in figure C.1 with the solution being time-independent the horizontal and vertical red lines never move. This asymmetric potential shape causes different energy levels to have different position expectation values seen in the green ($n = 0$) and blue ($n = 4$) lines though. Note that as the energy goes up the position expectation values get further away from the energy minimum.

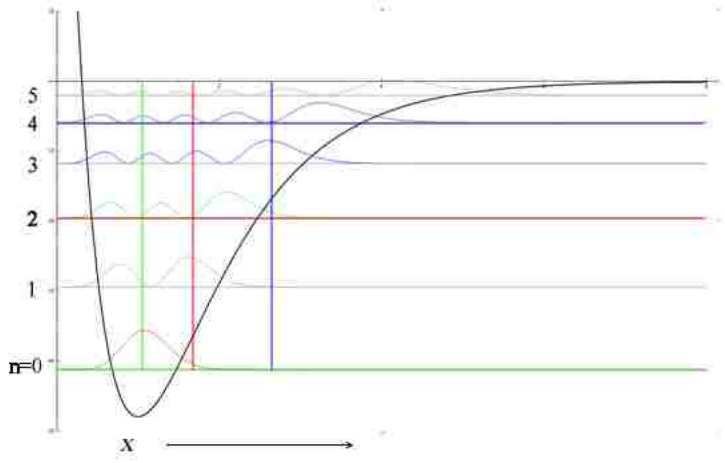

Figure C.2 Expectation values for energy and position in an anharmonic oscillator.

C.3 Dynamic Quantum States

It is more difficult to calculate quantum mechanics when the potential is time-dependent. This results in coherent behavior in the wave function. Stationary states are no longer the solution when the Hamiltonian includes time-dependent terms. This dependency produces eigenstates with time-dependent expectation values, or coherency. The Time-Dependent Schrodinger Equation (TDSE) is

$$i\hbar\frac{d}{dt}\Psi = \hat{H}\Psi. \tag{C.6}$$

In these calculations we must consider uncertainty between position, momentum, energy, and time.

Eqn. (C.7) is the general probability density solution to eqn. (C.6).

$$\Psi^*(x,t)\Psi(x,t) = \sum c_n^* c_n \psi_n^*(x)\psi_n(x) + \sum_m \sum_n c_m^* c_m \psi_m^*(x)\psi(x) e^{i2\pi \frac{E_m - E_n}{\hbar} t} \tag{C.7}$$

The first sum contains terms from the stationary state, time-independent solution. In quantum dynamics the second sum becomes non-zero revealing coherence.

C.4 Commutation Problems in Time

Here we demonstrate how a time-dependent Hamiltonian can come across commutativity issues. Consider the Hamiltonian for an oscillator influenced by an external field. Let's see if this Hamiltonian at time t_1 commutes with itself at any other time t_2.

$$\hat{H} = \hat{N} + \frac{1}{2}\hbar\omega + f(t)\hat{a} + f(t)\hat{a}^\dagger \tag{C.8}$$

$$\left[\hat{H}(t_1), \hat{H}(t_2)\right] = \left[\left(\hat{a}^\dagger\hat{a} + f(t_1)\hat{a} + f(t_1)\hat{a}^\dagger\right), \left(\hat{a}^\dagger\hat{a} + f(t_2)\hat{a} + f(t_2)\hat{a}^\dagger\right)\right] \tag{C.9}$$

$$= \left[\hat{a}^\dagger\hat{a}, f(t_2)\hat{a}\right] + \left[\hat{a}^\dagger\hat{a}, f(t_2)\hat{a}^\dagger\right] + 0 \tag{C.10}$$

$$+ \left[f(t_1)\hat{a}, \hat{a}^\dagger\hat{a}\right] + \left[f(t_1)\hat{a}, f(t_2)\hat{a}^\dagger\right] + 0 \tag{C.11}$$

$$+ \left[f(t_1)\hat{a}^\dagger, \hat{a}^\dagger\hat{a}\right] + \left[f(t_1)\hat{a}^\dagger, f(t_2)\hat{a}\right] + 0 \tag{C.12}$$

$$= \hat{a}\left(f(t_1) - f(t_2)\right) + \hat{a}^\dagger\left(f(t_2) - f(t_1)\right) \tag{C.13}$$

So we see in eqn. (C.14) that if the driving function is not constant through time than the Hamiltonian will not commute with itself at any other time.

$$\left[f(t_2) - f(t_1)\right]\left(\hat{a}^\dagger - \hat{a}\right) \neq 0 \tag{C.14}$$

C.5 The Baker Campbell Hausdorff formula

When comparing exponential structures of the form

$$e^A e^B = e^{A+B} \tag{C.15}$$

where A and B are operators, knowledge of the commutation relations between A and B is crucial. If the two operators commute then the above expression is correct. However, if the two operators do not commute then we end up with a more general form in eqn. (C.16).

$$e^A e^B = e^{A+B+\lambda} \tag{C.16}$$

where λ ensures the right terms cancel with the left terms upon expansion. Now if the commutator of the two operators commute with the operators then the following is true:

$$e^A e^B = e^{A+B+\frac{1}{2}[A,B]}. \tag{C.17}$$

We can also iterate this process for a product of many exponents

$$e^{V_1} e^{V_2} ... e^{V_N} = e^{i\sum_k V_k} e^{\frac{1}{2}\sum_{k,n}[V_k,V_n]} \tag{C.18}$$

For example, let $N = 3$ in eqn. (C.18):

$$e^{A_1} e^{A_2} e^{A_3} = e^{A_1+A_2+\frac{1}{2}[A_1,A_2]} e^{A_3} = e^{A_1+A_2+A_3} e^{\frac{1}{2}[A_1,A_2]+\frac{1}{2}[A_1,A_3]+\frac{1}{2}[A_2,A_3]}. \tag{C.19}$$

C.5.1 Commutation using the Cross-Product

For the next exercise, let us introduce a binary operation notation for the commutator. Given two operators P and Q we denote the product as:

$$P \times Q = [P,Q] = PQ - QP \tag{C.20}$$

This product is anticommutative, non-associative, and satisfies the Jacobi identity. Powers corresponding to this product are denoted in the usual way as nested commutators:

$$P \times (P \times Q) = [P,[P,Q]] \tag{C.21}$$

The Baker-Hausdorf formula can thus be written as:

$$e^{P\times}Q = e^{P}Qe^{-P} \tag{C.22}$$

C.5.2 Applying the Baker Campbell Hausdorff Formula and other tricks

For this dissertation we needed to rearrange: $i\dot{\alpha}_2 e^{\alpha_1 \hat{a}^\dagger}\hat{a}e^{-\alpha_1\hat{a}^\dagger}$ and $i\dot{\alpha}_3 e^{\alpha_1\hat{a}^\dagger}e^{\alpha_2\hat{a}}\hat{N}e^{-\alpha_2\hat{a}}e^{-\alpha_1\hat{a}^\dagger}$. To do this we use the BCH formula with cross-product antisymmetric product super-operator which is defined as

$$e^{X}Ye^{-X} = e^{X\times}Y. \tag{C.23}$$

The fact that since $\left[\hat{a}, \frac{\partial}{\partial\hat{a}}\right] \doteq -1$, $\left[\hat{a},\hat{a}^\dagger\right] \doteq 1$ allows us to say: $\hat{a}^\dagger \to -\frac{\partial}{\partial\hat{a}}$. This may be applied by seeing that if in general

$$e^{\gamma\frac{d}{dx}}f(x) = f(x+\gamma), \tag{C.24}$$

then

$$e^{-\alpha_1\frac{d}{d\hat{a}}\times}\hat{a} = \hat{a} - \alpha_1.$$

This brings the expression to

$$i\dot{\alpha}_2(\hat{a}-\alpha_1) + i\dot{\alpha}_3 e^{\alpha_1\hat{a}^\dagger\times}\left(e^{\alpha_2\hat{a}\times}\hat{N}\right). \tag{C.25}$$

Using an expansion we see the higher order terms vanish resulting in

$$e^{\alpha_2\hat{a}\times}\hat{N} \doteq \hat{N} + \alpha_2\hat{a}\times\hat{N}, \tag{C.26}$$

because $\hat{a}\times\left(\hat{a}\times\hat{N}\right) = 0$. We are thus able to construct a Schrodinger equation that is easily separable into isolated Lie algebraic parameter coefficients.

.

Appendix D

Lie Algebra and other Mathematical Tools

D.1 Deriving the Lie Algebra Details

Here we explicitly calculate the expressions associated with the Lie algebraic method needed for reference. Consider the transition probability from state n to m of a charged oscillator in a time-dependent dipole field.

$$\begin{aligned}
\langle m|\hat{U}|n\rangle &= \langle m| e^{\alpha_1 a^\dagger} e^{\alpha_2 a} e^{\alpha_3 N} e^{\alpha_4} |n\rangle \\
&= e^{\alpha_3 n} e^{\alpha_4} \langle m| e^{\alpha_1 a^\dagger} e^{\alpha_2 a} |n\rangle \\
&= e^{\alpha_3 n} e^{\alpha_4} \langle m| e^{\alpha_1 a^\dagger} e^{\alpha_2 a} \frac{1}{\sqrt{n!}} a^{\dagger n} |0\rangle \\
&= e^{\alpha_3 n} e^{\alpha_4} \left(e^{\alpha_1^* a} |m\rangle \right)^\dagger \frac{1}{\sqrt{n!}} e^{\alpha_2 \frac{\partial}{\partial a^\dagger}} a^{\dagger n} |0\rangle \\
&= e^{\alpha_3 n} e^{\alpha_4} \left(\frac{1}{\sqrt{m!}} \left(a^\dagger + \alpha_1 \right)^m |0\rangle \right)^\dagger \frac{1}{\sqrt{n!}} \left(a^\dagger + \alpha_2 \right)^n |0\rangle
\end{aligned} \tag{D.1}$$

Insert a binomial expression for cleanliness

$$\langle m|\hat{U}|n\rangle = e^{\alpha_3 n}e^{\alpha_4}\left(\frac{1}{\sqrt{m!}}\sum_{l=0}^{m}\binom{m}{l}\left(\hat{a}^\dagger\right)^{m-l}\alpha_1^{l*}|0\rangle\right)^\dagger\frac{1}{\sqrt{n!}}\sum_{k=0}^{n}\binom{n}{k}\left(\hat{a}^\dagger\right)^{n-k}\alpha_2^k|0\rangle$$

$$= e^{\alpha_3 n}e^{\alpha_4}\left(\frac{1}{\sqrt{m!}}\sum_{k=0}^{m}\binom{m}{k}\left(\hat{a}^\dagger\right)^{m-k}\alpha_1^k|0\rangle\right)^\dagger\frac{1}{\sqrt{n!}}\sum_{k=0}^{n}\binom{n}{k}\left(\hat{a}^\dagger\right)^{n-k}\alpha_2^k|0\rangle$$

$$= e^{\alpha_3 n}e^{\alpha_4}\frac{1}{\sqrt{m!}}\frac{1}{\sqrt{n!}}\sum_{k,l}\binom{m}{l}\binom{n}{k}\alpha_1^l\alpha_2^k\left(\left(\hat{a}^\dagger\right)^{m-l}|0\rangle\right)^\dagger\left(\hat{a}^\dagger\right)^{n-k}|0\rangle$$

$$= e^{\alpha_3 n}e^{\alpha_4}\frac{1}{\sqrt{m!}}\frac{1}{\sqrt{n!}}\sum_{k,l}\binom{m}{l}\binom{n}{k}\alpha_1^l\alpha_2^k\sqrt{(m-l)!}\sqrt{(n-k)!}\,\langle m-l|n-k\rangle$$

We let $l = m-n+k$, substitute in l, and collapse one sum

$$= e^{\alpha_3 n}e^{\alpha_4}\frac{1}{\sqrt{m!}}\frac{1}{\sqrt{n!}}\sum_{k}\binom{n}{k}\binom{m}{m-n+k}\alpha_1^{m-n+k}\alpha_2^k(n-k)!$$

$$= e^{\alpha_3 n}e^{\alpha_4}\frac{1}{\sqrt{m!}}\frac{1}{\sqrt{n!}}\sum_{k}\frac{n!}{k!\,(n-k)!}\frac{m!}{(m-n+k)!\,(m-(m-n+k))!}\alpha_1^{m-n+k}\alpha_2^k(n-k)!$$

Cleaning up binomials we get

$$= e^{\alpha_3 n}e^{\alpha_4}\sqrt{m!}\sqrt{n!}\sum_{k}\frac{1}{k!}\frac{1}{(m-n+k)!\,(n-k)!}\alpha_1^{m-n+k}\alpha_2^k.$$

We can now square the expression for the probability.

$$\left|\langle m|\hat{U}|n\rangle\right|^2 = \left|e^{\alpha_3 n}e^{\alpha_4}\sqrt{m!}\sqrt{n!}\sum_{k}\frac{1}{k!}\frac{1}{(m-n+k)!\,(n-k)!}\alpha_1^{m-n+k}\alpha_2^k\right|^2 \tag{D.2}$$

D.1.1 Ladder Operator Expectation Values

Here we find the expectation values of the position and momentum operators in arbitrary state $|n\rangle$ using the Lie algebraic method. The relationship between position/momentum and ladder operators is

$$\begin{array}{|c|c|}\hline \hat{x}=\sqrt{\frac{\Omega(s)}{2m}}\left(\hat{a}^{\dagger}+\hat{a}\right) & \hat{p}_x=-i\frac{\partial}{\partial x}=i\sqrt{\frac{m\Omega(s)}{2}}\left(\hat{a}^{\dagger}-\hat{a}\right) \\ \hline \hat{a}=\sqrt{\frac{m\Omega(s)}{2}}\left(\hat{x}+\frac{i}{m\Omega(s)}\hat{p}_x\right) & \hat{a}^{\dagger}=\sqrt{\frac{m\Omega(s)}{2}}\left(\hat{x}-\frac{i}{m\Omega(s)}\hat{p}_x\right) \\ \hline \end{array}.$$

We begin by finding $\langle\hat{a}\rangle$ with

$$\langle n|\hat{U}^{-1}\hat{a}\hat{U}|n\rangle=\langle n|e^{-\alpha_4}e^{-\alpha_3\hat{N}}e^{-\alpha_2\hat{a}}e^{-\alpha_1\hat{a}^{\dagger}}\hat{a}e^{\alpha_1\hat{a}^{\dagger}}e^{\alpha_2\hat{a}}e^{\alpha_3\hat{N}}e^{\alpha_4}|n\rangle. \tag{D.3}$$

$e^{-\alpha_4}$ commutes with everything so

$$\begin{aligned}\langle n|\hat{U}^{-1}\hat{a}\hat{U}|n\rangle&=\langle n|\left(e^{-\alpha_3\hat{N}\times}\left(e^{-\alpha_2\hat{a}\times}\left(e^{-\alpha_1\hat{a}^{\dagger}\times}\hat{a}\right)\right)\right)|n\rangle\\&=\langle n|\left(e^{-\alpha_3\hat{N}\times}\left(e^{-\alpha_2\hat{a}\times}\left(\hat{a}+\alpha_1\right)\right)\right)|n\rangle\\&=\langle n|\left(e^{-\alpha_3\hat{N}\times}\left(\hat{a}+\alpha_1\right)\right)|n\rangle\\&=\langle n|\left(\hat{a}e^{\alpha_3}+\alpha_1\right)|n\rangle=\alpha_1\surd\end{aligned} \tag{D.4}$$

Now find $\left\langle\hat{a}^{\dagger}\right\rangle$

$$\begin{aligned}\langle n|\hat{U}^{-1}\hat{a}^{\dagger}\hat{U}|n\rangle&=\langle n|e^{-\alpha_4}e^{-\alpha_3\hat{N}}e^{-\alpha_2\hat{a}}e^{-\alpha_1\hat{a}^{\dagger}}\hat{a}^{\dagger}e^{\alpha_1\hat{a}^{\dagger}}e^{\alpha_2\hat{a}}e^{\alpha_3\hat{N}}e^{\alpha_4}|n\rangle\\&=\langle n|\left(e^{-\alpha_3\hat{N}\times}\left(e^{-\alpha_2\hat{a}\times}\left(e^{-\alpha_1\hat{a}^{\dagger}\times}\hat{a}^{\dagger}\right)\right)\right)|n\rangle\\&=\langle n|\left(e^{-\alpha_3\hat{N}\times}\left(e^{-\alpha_2\hat{a}\times}\hat{a}^{\dagger}\right)\right)|n\rangle\\&=\langle n|\left(e^{-\alpha_3\hat{N}\times}\left(e^{-\alpha_2\hat{a}\times}\hat{a}^{\dagger}\right)\right)|n\rangle\\&=\langle n|\left(e^{-\alpha_3\hat{N}\times}\left(\hat{a}^{\dagger}-\alpha_2\right)\right)|n\rangle\\&=\langle n|\left(\hat{a}^{\dagger}e^{-\alpha_3}-\alpha_2\right)|n\rangle\end{aligned} \tag{D.5}$$

$$\left\langle\hat{a}^{\dagger}\right\rangle=-\alpha_2\surd$$

Therefore

$$\langle \hat{x} \rangle = \sqrt{\frac{1}{2m\omega}} (\alpha_1 - \alpha_2) \qquad \text{and} \qquad \langle \hat{p} \rangle = -i\sqrt{\frac{m\omega}{2}} (\alpha_1 + \alpha_2).$$

D.1.2 Harmonic Algebra Wei-Norman Coefficients

To find $\hat{U}$ for a harmonic system consider the Lie Algebra with elements $\left\{\hat{a}^\dagger, \hat{a}, \hat{N}, 1\right\}$. The Wei Norman Ansatz in normal ordering is

$$\hat{U}(t) = e^{\alpha_1 \hat{a}^\dagger} e^{\alpha_2 \hat{a}} e^{\alpha_3 \hat{N}} e^{\alpha_4} \tag{D.6}$$

where the functions $\alpha_i(t)$ are time-dependent. Invert the operator equation

$$i\frac{d\hat{U}}{dt}\hat{U}^{-1} \doteq \hat{H}(t) \tag{D.7}$$

where $\hat{U}^{-1} = e^{-\alpha_4} e^{-\alpha_3 \hat{N}} e^{-\alpha_2 \hat{a}} e^{-\alpha_1 \hat{a}^\dagger}$ and expand it into 4 terms.

$$\begin{aligned} i\left(\frac{d}{dt} e^{\alpha_1 \hat{a}^\dagger} e^{\alpha_2 \hat{a}} e^{\alpha_3 \hat{N}} e^{\alpha_4}\right) e^{-\alpha_4} e^{-\alpha_3 \hat{N}} e^{-\alpha_2 \hat{a}} e^{-\alpha_1 \hat{a}^\dagger} &= i\dot{\alpha}_1 \hat{a}^\dagger \hat{U}\hat{U}^{-1} \\ &+ i\dot{\alpha}_2 e^{\alpha_1 \hat{a}^\dagger} a e^{\alpha_2 \hat{a}} e^{\alpha_3 \hat{N}} e^{\alpha_4} e^{-\alpha_4} e^{-\alpha_3 \hat{N}} e^{-\alpha_2 \hat{a}} e^{-\alpha_1 \hat{a}^\dagger} \\ &+ i\dot{\alpha}_3 e^{\alpha_1 \hat{a}^\dagger} e^{\alpha_2 \hat{a}} N e^{\alpha_3 \hat{N}} e^{\alpha_4} e^{-\alpha_4} e^{-\alpha_3 \hat{N}} e^{-\alpha_2 \hat{a}} e^{-\alpha_1 \hat{a}^\dagger} \\ &+ i\dot{\alpha}_4 \hat{U}\hat{U}^{-1} \end{aligned} \tag{D.8}$$

Note that the motivation of the inversion is purely algebraic. Upon inspection this quickly collapses to

$$= i\dot{\alpha}_1 \hat{a}^\dagger + i\dot{\alpha}_2 e^{\alpha_1 \hat{a}^\dagger} \hat{a} e^{-\alpha_1 \hat{a}^\dagger} + i\dot{\alpha}_3 e^{\alpha_1 \hat{a}^\dagger} e^{\alpha_2 \hat{a}} \hat{N} e^{-\alpha_2 \hat{a}} e^{-\alpha_1 \hat{a}^\dagger} + i\dot{\alpha}_4.$$

Applying Appendix (C.5.2) we get to the middle two terms and we get

$$i\frac{d\hat{U}}{dt}\hat{U}^{-1} = i\dot{\alpha}_1 \hat{a}^\dagger + i\dot{\alpha}_2 (\hat{a} - \alpha_1) + i\dot{\alpha}_3 e^{\alpha_1 \hat{a}^\dagger \times} \left(e^{\alpha_2 \hat{a} \times} \hat{N}\right) + i\dot{\alpha}_4. \tag{D.9}$$

Next we find, $e^{\alpha_2 \hat{a} \times} \hat{N} \doteq \hat{N} + \alpha_2 \hat{a} \times \hat{N} + \frac{\alpha^2}{2} \hat{a} \times \left(\hat{a} \times \hat{N}\right) + \ldots$ but run into $\hat{a} \times \left(\hat{a} \times \hat{N}\right) = 0$, this looks like:

$$i\frac{d\hat{U}}{dt}\hat{U}^{-1} = i\dot{\alpha}_1 \hat{a}^\dagger + i\dot{\alpha}_2 (\hat{a} - \alpha_1) + i\dot{\alpha}_3 e^{\alpha_1 \hat{a}^\dagger \times} \left(\hat{N} + \alpha_2 \hat{a} \times \hat{N}\right) + i\dot{\alpha}_4 \tag{D.10}$$

$$= i\dot{\alpha}_1\hat{a}^\dagger + i\dot{\alpha}_2(\hat{a}-\alpha_1) + i\dot{\alpha}_3 e^{\alpha_1\hat{a}^\dagger\times}\hat{N} + i\dot{\alpha}_3\alpha_2 e^{\alpha_1\hat{a}^\dagger\times}\left(\hat{a}\times\hat{N}\right) + i\dot{\alpha}_4 \tag{D.11}$$

$$= i\dot{\alpha}_1\hat{a}^\dagger + i\dot{\alpha}_2(\hat{a}-\alpha_1) + i\dot{\alpha}_3 a^\dagger(\hat{a}-\alpha_1) + i\dot{\alpha}_3\alpha_2(\hat{a}-\alpha_1) + i\dot{\alpha}_4 \tag{D.12}$$

This gives us the standard Lie algebraic form in eqn. (C.37) which we can equate to any Hamiltonian composed of Lie Algebra with elements $\left\{\hat{a}^\dagger,\hat{a},\hat{N},1\right\}$ and retrieve the desired 4 differential equations-of-motion.

$$\hat{H} = i\frac{d\hat{U}}{dt}\hat{U}^{-1} = i(\dot{\alpha}_1 - \dot{\alpha}_3\alpha_1)\hat{a}^\dagger + i(\dot{\alpha}_2 + \dot{\alpha}_3\alpha_2)\hat{a} + i(\dot{\alpha}_3)\hat{N} + i(\dot{\alpha}_4 - \dot{\alpha}_3\alpha_2\alpha_1 - \dot{\alpha}_2\alpha_1)1 \tag{D.13}$$

The RHS of eqn. (C.37) agrees with the computer algebra done in the program from A.4.

D.1.3 Anharmonic Algebra Wei-Norman Coefficients

When considering anharmonic potentials for the quantized variable, it is necessary to add an element to the algebra we used in the harmonic case. Using the Wei-Norman Ansatz for this higher order algebra be write,

$$\hat{U}(t) = e^{\alpha_1\hat{a}^\dagger}e^{\alpha_2\hat{a}}e^{\alpha_3\hat{N}}e^{\alpha_4\hat{N}^2}e^{\alpha_5}. \tag{D.14}$$

We begin by inverting eqn. (C.38) in the Time-Dependent Schrodinger Equation for the Time-Evolution operator, $i\left(\frac{d}{dt}\hat{U}\right)\hat{U}^{-1} = \hat{H}$ to get

$$i\left(\frac{d}{dt}e^{\alpha_1\hat{a}^\dagger}e^{\alpha_2\hat{a}}e^{\alpha_3\hat{N}}e^{\alpha_4\hat{N}^2}e^{\alpha_5}\right)e^{\alpha_1\hat{a}^\dagger}e^{\alpha_2\hat{a}}e^{\alpha_3\hat{N}}e^{\alpha_4\hat{N}^2}e^{\alpha_5} = \hat{H}, \tag{D.15}$$

The motivation of the inversion is purely algebraic as it sets the equation up for matching coefficients of the Lie algebra elements. Equating coefficients of the 5 Lie algebra elements in eqn. (C.39) we expect 5 non-linear coupled equations for the αs. The LHS separated into terms collapses to a landmark point in our calculation of

$$i\dot{\alpha}_1\hat{a}^\dagger + i\dot{\alpha}_2 e^{\alpha_1\hat{a}^\dagger}\hat{a}e^{-\alpha_1\hat{a}^\dagger} + i\dot{\alpha}_3 e^{\alpha_1\hat{a}^\dagger}e^{\alpha_2\hat{a}}\hat{N}e^{-\alpha_2\hat{a}}e^{-\alpha_1\hat{a}^\dagger} + i\dot{\alpha}_4 e^{\alpha_1\hat{a}^\dagger}e^{\alpha_2\hat{a}}\hat{N}^2e^{-\alpha_2\hat{a}}e^{-\alpha_1\hat{a}^\dagger} + i\dot{\alpha}_5. \tag{D.16}$$

The inside three terms we use the Baker-Hausdorff formula with cross-product antisymmetric product super operators $e^X Y e^{-X} = e^{X\times}Y$ rewritten as

$$i\left(\frac{d}{dt}\hat{U}\right)\hat{U}^{-1} = i\dot{\alpha}_1\hat{a}^\dagger + i\dot{\alpha}_2 e^{\alpha_1\hat{a}^\dagger\times}\hat{a} + i\dot{\alpha}_3 e^{\alpha_1\hat{a}^\dagger\times}\left(e^{\alpha_2\hat{a}\times}\hat{N}\right) + i\dot{\alpha}_4 e^{\alpha_1\hat{a}^\dagger\times}\left(e^{\alpha_2\hat{a}\times}\hat{N}^2\right) + i\dot{\alpha}_5 \quad \text{(D.17)}$$

Now with the help of the computer algebra system we get

$$= i\dot{\alpha}_1\hat{a}^\dagger + i\dot{\alpha}_2\left(\hat{a} - \alpha_1\right) + i\dot{\alpha}_3\left(\hat{N} - \alpha_1\hat{a}^\dagger + \alpha_2\hat{a} - \alpha_1\alpha_2\right) +$$
$$i\dot{\alpha}_4\left(\hat{N}^2 - 2\alpha_1\hat{a}^\dagger\left\langle\hat{N}\right\rangle + 2\alpha_2\hat{a}\left\langle\hat{N}\right\rangle - 2\alpha_1\alpha_2\left\langle\hat{N}\right\rangle\right) + i\dot{\alpha}_5$$

$$= \left(i\dot{\alpha}_1 - i\alpha_1\dot{\alpha}_3 - i2\alpha_1\dot{\alpha}_4\left\langle\hat{N}\right\rangle\right)\hat{a}^\dagger + \left(i\dot{\alpha}_4 2\alpha_2\left\langle\hat{N}\right\rangle + i\dot{\alpha}_2 + i\dot{\alpha}_3\alpha_2\right)\hat{a} + \left(i\dot{\alpha}_3\right)\hat{N} + \left(i\dot{\alpha}_4\right)\hat{N}^2 +$$
$$\left(i\dot{\alpha}_5 - i\dot{\alpha}_4 2\alpha_1\alpha_2\left\langle\hat{N}\right\rangle - i\dot{\alpha}_3\alpha_1\alpha_2 - i\dot{\alpha}_2\alpha_1\right)1$$

D.2 Natural Coordinate Transformations

To begin a simple derivation of natural coordinates [16] we start with the coordinates used in the reactant channel. For these reactant channel coordinates we take the B and C atoms to be bound and the interaction between A and C to be negligible. We may reduce the problem to two dimensions using the following reduced mass coordinates x and y depicted in figure D.3.

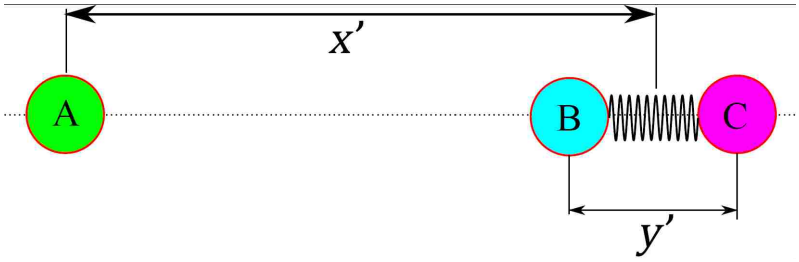

Figure D.1 Collinear coordinates for the reactants.

Note that the center-of-mass coordinate has been removed. Now when we transform the Hamiltonian, we can ignore the kinetic energy of the center-of-mass to get

$$H_\mathrm{r} = \frac{p_x^2}{2\mu} + \frac{p_y^2}{2m} + V_\mathrm{BC}\left(x\right) + V_\mathrm{AB}\left(y - \frac{\mu}{m_\mathrm{B}}x\right) \quad \text{(D.18)}$$

where $\mu = \frac{m_B m_C}{m_B + m_C}$ $m = \frac{m_A(m_B+m_C)}{M}$ $M = m_A + m_B + m_C$.

Since we are considering a reaction we may also express the atomic positions in terms of a product coordinate system seen in figure D.4.

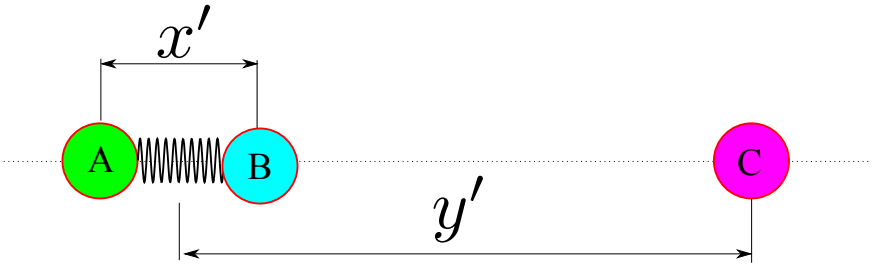

Figure D.2 Collinear coordinates for the products.

where the same Hamiltonian may be expressed in the new variables x' and y' as

$$H_p = \frac{p_{x'}^2}{2\mu'} + \frac{p_{y'}^2}{2m'} + V_{AB}\left(x'\right) + V_{BC}\left(y' - \frac{\mu'}{m_B}x'\right), \tag{D.19}$$

where the masses take on the new form $\mu' = \frac{m_A m_B}{m_A + m_B}$ $m' = \frac{(m_A+m_B)m_C}{M}$.

The coordinates are defined as follows: x and x' are the distances between the nuclei in the diatomic molecule. y and y' are the distances between the atom and the diatomic molecule's center-of-mass. Natural coordinates are designed to pass smoothly from the reactant coordinates to the product coordinates. The origin of these natural coordinates comes from "wrapping" the Morse potential reaction function into a curved function of r and mass scaled vibrational coordinates seen in figure D.5.

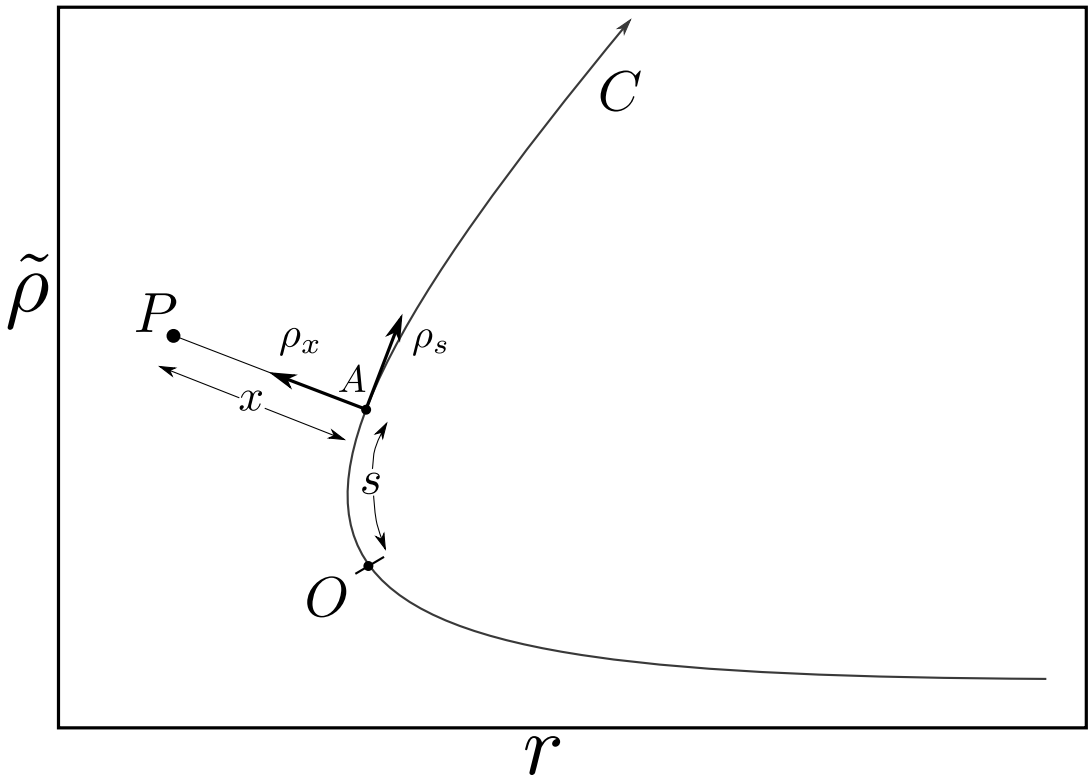

Figure D.3 Curvillinear coordinates and the Frenet frame.

M.S. Child et. al. derive this through a series of orthogonal and canonical transformations. The result is a clean kinetic energy term allowing the Hamiltonian to be expressed in terms of the dihedral coordinates s and x classically as

$$H = \frac{1}{2m}\left(\frac{1}{\eta^2}P_s^2 + P_x^2\right) + V(s,x), \tag{D.20}$$

where

$$\eta = 1 + \kappa(s)x \tag{D.21}$$

and $\kappa(s)$ is a curvature function describing the shape of the reaction coordinate as you move along the translational degree-of-freedom. For a thorough derivation we choose to compare directly to M.S. Child[16] and let $x \to \rho$, $y \to r$ and $x' \to \rho'$, $y' \to r'$. The reactant and product coordinates

are then related through the transformation given in eqn. (C.51).

$$\begin{pmatrix} r' \\ \rho' \end{pmatrix} = \begin{pmatrix} -\frac{m_A}{m_A+m_B} & -\frac{m_B M}{(m_A+m_B)(m_B+m_C)} \\ -1 & \frac{m_C}{m_B+m_C} \end{pmatrix} \begin{pmatrix} r \\ \rho \end{pmatrix} \tag{D.22}$$

To keep the single mass "bobsled" dynamic interpretation we need to reduce the kinetic energy to be for a single mass. It is therefore necessary to reduce the kinetic energy to a form invariant to any orthogonal transformation on $(r,\tilde{\rho})$. Starting with the reactant channel (eqn. (6.47)) we get:

$$T = \frac{1}{2}m\dot{r}^2 + \frac{1}{2}\mu\dot{\rho}^2 \rightarrow \frac{1}{2}m\left(\dot{r}^2 + \dot{\tilde{\rho}}\right) = \frac{1}{2m}\left(p_r^2 + p_{\tilde{\rho}}^2\right) \tag{D.23}$$

where

$$\tilde{\rho} = \sqrt{\frac{\mu}{m}}\rho. \tag{D.24}$$

We are then able to see the asymptotes (reactant and product channels) of this skewed coordinate system are given by

$$\begin{cases} \tilde{\rho} = 0 & \Longrightarrow r_A \rightarrow \infty \\ \tilde{\rho} = \sqrt{\frac{M m_B}{m_A m_C}}\, r & \Longrightarrow r_C \rightarrow \infty \end{cases} \tag{D.25}$$

A similar scaling on the product side, designed to accommodate the change in translational reduced mass yields

$$\tilde{r}' = \sqrt{\frac{m'}{m}}\, r \qquad \tilde{\rho}' = \sqrt{\frac{\mu'}{m}}\,\rho' \tag{D.26}$$

which are orthogonal transformations of $(r,\tilde{\rho})$. This method introduces an angle of skew,

$$\chi = \tan^{-1}\sqrt{\frac{M m_B}{m_A m_C}}. \tag{D.27}$$

This angle allows us to express the whole transformation as:

$$\begin{pmatrix} \tilde{r}' \\ \tilde{\rho}' \end{pmatrix} = \begin{pmatrix} \cos\chi & \sin\chi \\ \sin\chi & -\cos\chi \end{pmatrix} \begin{pmatrix} r \\ \tilde{\rho} \end{pmatrix}. \tag{D.28}$$

T may then be expressed for the whole reaction as:

$$T = \frac{1}{2m}\left(\dot{\tilde{r}}'^2 + \dot{\tilde{\rho}}'^2\right) = \frac{1}{2m}\left(p_{\tilde{r}'}^2 + p_{\tilde{\rho}'}^2\right). \tag{D.29}$$

The coordinates of a point P in this system are precisely defined by the distance perpendicular to the path x, and the distance along the path s. By this definition the *Cartesian coordinates* $(r,\tilde{\rho})$ at point P in figure A.5 , abbreviated $\vec{r}$, may be written

$$\vec{r} = \vec{a} + x\vec{\rho}_x \tag{D.30}$$

and the dihedral $(\vec{\rho}_s, \vec{\rho}_x)$ is tied to the plane curve C by the Frenet formula

$$\frac{d\vec{\rho}_x}{ds} = \kappa\vec{\rho}_s \tag{D.31}$$

linking the change $\vec{\rho}_x$to the curvature $\kappa(s)$ of C, and the requirement that as the dihedral moves along the path

$$\frac{d\vec{a}}{ds} = \vec{\rho}_s. \tag{D.32}$$

The next step is to determine the momenta (P_s, P_x) conjugate to (s,x), for which purpose we use a classical generator of the form

$$F_3 = -\vec{p}\cdot\vec{r} = -\vec{p}\cdot(\vec{a} + x\vec{\rho}_x) \tag{D.33}$$

so that in light of the above two first order differential equations

$$P_s = -\frac{\partial F_3}{\partial s} = \vec{p} \cdot \left(\frac{\partial \vec{a}}{\partial s} + x \frac{\partial \vec{\rho}_x}{\partial s} \right) = (1 + \kappa x)\, \vec{p} \cdot \vec{\rho}_s = (1 + \kappa x)\, \vec{p}_s \tag{D.34}$$

$$P_x = -\frac{\partial F_3}{\partial x} = \vec{p} \cdot \vec{\rho}_x = p_x \tag{D.35}$$

Here we distinguish between the new conjugate momenta (P_s, P_x) and the components (p_s, p_x) of the old linear momentum $\vec{p}$ along $(\vec{\rho}_s, \vec{\rho}_x)$. It remains to note that (p_s, p_x) may be obtained by an orthogonal transformation of $\left(p_r, p_{\tilde{\rho}}\right)$ in the kinetic energy, hence

$$T = \frac{1}{2m} \left(p_s^2 + p_x^2 \right) = \frac{1}{2m} \left(\frac{1}{(1 + \kappa x)^2} P_s^2 + P_x^2 \right) \tag{D.36}$$

which is the kinetic part of eqn. (C.49).

Bibliography

[1] B. Yang, K. Han, and S. Ding, "Application of dynamical Lie algebraic method to atom-diatomic molecule scattering," J. Math. Chem. **28,** 247 (2000).

[2] D. Rapp and T. Kassal, "Exact Quantum-Mechanical Calculation of Vibrational Energy Transfer to an Oscillator by Collision with a Particle," J. Chem. Phys. **48,** 5287 (1968).

[3] G. Drake and C. Lin, "Semiclassical study of the vibrational excitation of H_2, in collision with He," J. Phys. B: Atom. Molec. Phys. **7,** 398 (1974).

[4] R. D. Santiago, O. Alvarez-Bajo, R. Lemus, J. M. Arias, J. Gomez-Camacho, and M. Rodriguez-Gallardo, "Algebraic description of the inelastic collision between an atom and a Morse oscillator in one dimension," J. Phys. B: At., Mol. Phys. **41,** 145203 (2008).

[5] O. Skrebkov and A. Smirnov, "Classical dynamics of vibrational-translational energy transfer in linear collisions of an atom and a diatomic molecule/anharmonic oscillator," Chemical Physics **198,** 287 (1995).

[6] D. J. Locker and D. J. Wilson, "Reactive Scattering. A Simple Three-Body Model," The J. of Chem. Phys. **53,** 2858 (1970).

[7] E. Merzbacher, *Quantum Mechanics (third edn.)*, 3rd ed. (Wiley, 1997).

[8] M. Berrondo and J. Recamier, "Dipole induced transitions in an anharmonic oscillator: A dynamical mean field model," Chem. Phys. Lett. **503,** 180 (2010).

[9] J. Wei and E. Norman, "Lie Algebraic Solution of Linear Differential Equations," J. Math. Phys. **4,** 575 (1963).

[10] J. Recamier and W. Mochan, "Energy transfer to an anharmonic diatomic system," Mol. Phys. **107,** 1467 (2009).

[11] B. Gazdy and D. Micha, "The linearly driven parametric oscillator: Application to collisional energy transfer," J. Chem. Phys. **82,** 4926 (1985).

[12] D. Rapp, "Complete Classical Theory of Vibrational Energy Exchange," J. Chem. Phys. **32,** 735 (1960).

[13] J. Recamier, "An algebraic method for the study of collisions with an anharmonic oscillator," Intl. J. Quantum Chem. **24,** 655 (1990).

[14] M. Child, *Molecular Collision Theory* (Dover, 1996), pp. 210–234.

[15] D. Secrest and B. Johnson, "Exact Quantum-Mechanical Calculation of a Collinear Collision of a Particle with a Harmonic Oscillator," J. Chem. Phys. **45,** 4556 (1966).

[16] G. Daren, Y. Xizhang, D. Shiliang, Y. Benhui, and H. Dongming, "A dynamical Lie algebraic method for quantum reactive scattering," Science in China (Series B) **45,** 460 (1998).

[17] A. Clark and A. Dickinson, "Collinear collision of an atom and a Morse oscillator: exact quantum mechanical results," J. Phys. B: At. Mol. Phys. **6,** 164 (1973).

[18] R. Marcus, "On the Analytical Mechanics of Chemical Reactions. Classical Mechanics of Linear Collisions," J. Chem. Phys. **45,** 4500 (1966).

[19] K. G. Kay, "Normal collision coordinates for collinear triatomic systems," Mol. Phys. **27,** 809 (1974).

[20] J. Hirschfelder, "Coordinates which diagonalize the kinetic energy of relative motion," Intern. J. Quantum Chem. **3,** 17 (1969).

[21] P. Morse, "Diatomic Molcules According to the Wave Mechanics. II. Vibrational Levels," Phys. Rev. **34,** 57 (1929).

[22] M. Berrondo and A. Palma, "The algebraic approach to the Morse oscillator," J. Phys. A: Math. Gen. **13,** 773 (1980).

[23] F. Iachello and R. Levine, *Algebraic Theory of Molecules* (Oxford University Press, 1995).

[24] M. H. Mok and J. C. Polanyi, "Location of Energy Barriers. II. Correlation with Barrier Height," J. Chem. Phys. **51,** 1451 (1969).

[25] A. H. Zewail, "Femtochemistry: Recent Progress in Studies of Dynamics and Control of Reactions and Their Transition States," J. Phys. Chem. **100,** 12701 (1996).

Index